

---

Structural analysis and regional interpretation of the Sprigg Inlet  
Shear Zone, with implications for the tectonic evolution  
of the Fleurieu Arc.

---

Glen Buick, B.Sc.



This thesis is submitted as partial fulfilment of the requirements for the  
Honours Degree of Bachelor of Science in Geology

University of Adelaide

November 2000

Australian National Grid Reference  
Barker sheet 1:250 000 54-13  
PTS 6426 – 1 & 2 (1:50 000)  
PTS 6526 – 3 & 4 (1:50 000)

## ABSTRACT

The Dudley Peninsula lies directly within the hinge of the Fleurieu Arc, a recess developed during the Cambro-Ordovician Delamerian Orogeny. On Dudley Peninsula, the structural grain was previously defined to bend through  $50^\circ$ , as defined by the regional trace of the Sprigg Inlet Shear Zone. A structural analysis of the Sprigg Inlet Shear Zone revealed structural features recording two deformation events. The initial and most intense deformation resulted in top to the WNW directed transpression, which involved a dextral strike-slip component. The second deformation involved sinistral strike-slip shear and resulted in the formation of a crenulation and folded boudins along-strike. Interpretation of magnetic data from Dudley Peninsula, along with mapping on the south coast of Dudley Peninsula has revealed that the structural grain on Dudley Peninsula does not define a major ( $\sim 50^\circ$ ) bend as previously proposed. A slight ( $\sim 5^\circ$ - $10^\circ$ ) bend of folds, faults and the Sprigg Inlet Shear Zone occurs between the NE coast and western part of Dudley Peninsula. This renewed interpretation is continuous with structural features on the limbs of the Fleurieu Arc, on southern Fleurieu Peninsula and western Kangaroo Island. This bend formed due to impingement of sediments onto the SE corner of the Gawler Craton during NW directed compression. The Fleurieu Arc is therefore classified as a Primary Arc, which possibly involved a small component of oroclinal bending during a late northerly directed compression active on Kangaroo Island either, late in, or post-dating the first phase of the Delamerian Orogeny.

## TABLE OF CONTENTS

Page no.

### **Abstract**

### **List of figures and maps**

### **1 - Introduction**

|   |   |
|---|---|
| 1.1 – Location of the Dudley Peninsula within the Fleurieu Arc..... | 1 |
| 1.2 – Aims and methods.....   | 5 |

### **2 - Geological Overview**

|  |   |
|--|---|
| 2.1– Stratigraphy on Dudley Peninsula..... | 7 |
| 2.2 – Structure of the Fleurieu Arc.....   | 8 |
| 2.3 – Deformation of the SAFTB.....        | 9 |

### **3 - Geology of the Dudley Peninsula**

|  |    |
|--|----|
| 3.1 – Structural analysis of the NE coast of Dudley Peninsula..... | 10 |
| 3.1.1 – Domain 1 – The Cuttlefish Bay Anticline (CBA).....         | 15 |
| 3.1.2 – Domain 2 – The Sprigg Inlet Shear Zone (SISZ)...           | 17 |
| 3.1.3 – Domain 3 – The Snapper Point Homoclinal Zone (SPHZ).....   | 27 |
| 3.1.4 – Domain 4 – The Dudley Fault Zone (DFZ).....                | 29 |
| 3.2 – Charlies Gulch Region.....                                   | 31 |

### **4 - Analysis of boudin, vein and fold geometries**

|                            |    |
|----------------------------|----|
| 4.1 – Boudin Analysis..... | 33 |
| 4.2 – Vein Analysis.....   | 36 |
| 4.3 – Fold Analysis.....   | 41 |
| 4.4 – Discussion.....      | 42 |

### **5 - Magnetic Interpretation of Dudley Peninsula.....**

### **6 – Discussion**

|   |    |
|---|----|
| 6.1 – Regional comparisons.....         | 51 |
| 6.2 – Movements during deformation..... | 53 |

|  |           |
|--|-----------|
| 6.3 – Tectonic models.....                   | 54        |
| <b>7 – Conclusions</b> .....                 | <b>58</b> |
| <b>Acknowledgements</b> .....                | <b>59</b> |
| <b>References</b> .....                      | <b>60</b> |
| <b>Appendix 1 – Boudinage analysis</b> ..... | <b>65</b> |
| <b>Appendix 2 – Fold analysis</b> .....      | <b>67</b> |
| <b>Thin section descriptions</b> .....       | <b>69</b> |

## LIST OF FIGURES

- Figure 1** – Location map.
- Figure 2** – Cross-section sketch of outcrop 200 m north of Cuttlefish Bay.
- Figure 3** – Cartoons showing the orientation of the representative finite strain ellipsoid within the Sprigg Inlet Shear Zone.
- Figure 4** – Photo of interbedded metapelites and metapsammites from the Sprigg Inlet Shear Zone.
- Figure 5** – Thin section photograph showing crenulation within the Sprigg Inlet Shear Zone.
- Figure 6** – Thin section photo and cartoon representation of andalusite/staurolite porphyroblast within the Sprigg Inlet Shear Zone.
- Figure 7** – Array of structures within the Sprigg Inlet Shear Zone.
- Figure 8** – Photos of boudin types within the Sprigg Inlet Shear Zone.
- Figure 9** – Photo showing vein styles within the Sprigg Inlet Shear Zone.
- Figure 10** – Photo showing contorted metapsammite near the SE boundary of the Sprigg Inlet Shear Zone.
- Figure 11** – Field outcrop and hand specimen photo of laminated actinolite/cordierite rich hornfels from the NW boundary of the Sprigg Inlet Shear Zone.
- Figure 12** – Map of Charlies Gulch region.
- Figure 13** – Measurements of quartzite boudins used in boudinage reconstruction.
- Figure 14** – Theoretical representation of shearband-type boudin development within the Sprigg Inlet Shear Zone.
- Figure 15** – Representative diagram of sigmoidal interboudin vein fill.
- Figure 16** – Cartoons showing stress conditions during formation of *en-echelon* vein sets within the Sprigg Inlet Shear Zone, (Mechanism 1).
- Figure 17** – Cartoon model showing formation of *en-echelon* vein sets during progressive simple shear, (mechanism 2).
- Figure 18** – Stereographic projection showing theoretical vein rotation.

**Figure 19** – Cartoons showing stress conditions active during formation of conjugate vein arrays within the Sprigg Inlet Shear Zone, (mechanism 3).

**Figure 20** – Magnetic interpretation of Dudley Peninsula.

**Figure 21** – Renewed interpretation of structural features on eastern Kangaroo Island with comparisons to structural features on southern Fleurieu Peninsula.

**Figure 22** – Tectonic model showing development of the Fleurieu Arc.

---

---

## 1 INTRODUCTION

### 1.1 Location of the Dudley Peninsula within the Fleurieu Arc

The Dudley Peninsula is a 35 km wide headland on eastern Kangaroo Island, located about 150 km south of Adelaide. The island is separated from the mainland by Backstairs Passage, a 10 km wide sea channel which separates the Dudley Peninsula from the Fleurieu Peninsula on Mainland Australia. A narrow 1-2 km land-bridge of aeolian dunes connects Dudley Peninsula to the western part of Kangaroo Island.

Rock units and structures are, to a certain degree, continuous from Dudley Peninsula through to the Fleurieu Peninsula. Although a definite comparison between structures from the two areas has yet to be achieved. Geologically the Dudley Peninsula lies within part of the Southern Adelaide Fold-Thrust Belt (SAFTB) (fig. 1).

Within the SAFTB, asymmetric low-grade shear zones with associated basal imbricate thrusts are common (Yassaghi et al. 2000). These shear zones and associated thrusts along with cleavage, bedding, and fold axial traces define the structural grain of the SAFTB. The structural grain of the SAFTB shows a near 90° bend in plan view, from N-S near Adelaide to generally E-W on western Kangaroo Island (fig. 1). This bend is referred to as the syntaxial (concave to the NW) Fleurieu Arc (Marshak and Flottmann, 1996).

The regional traces of folds, faults, and foliations define a plan view bend in many fold-thrust belts around the world (Marshak, 1988). A classification system has been developed which separates these bent orogens into types indicative of their mode of formation.

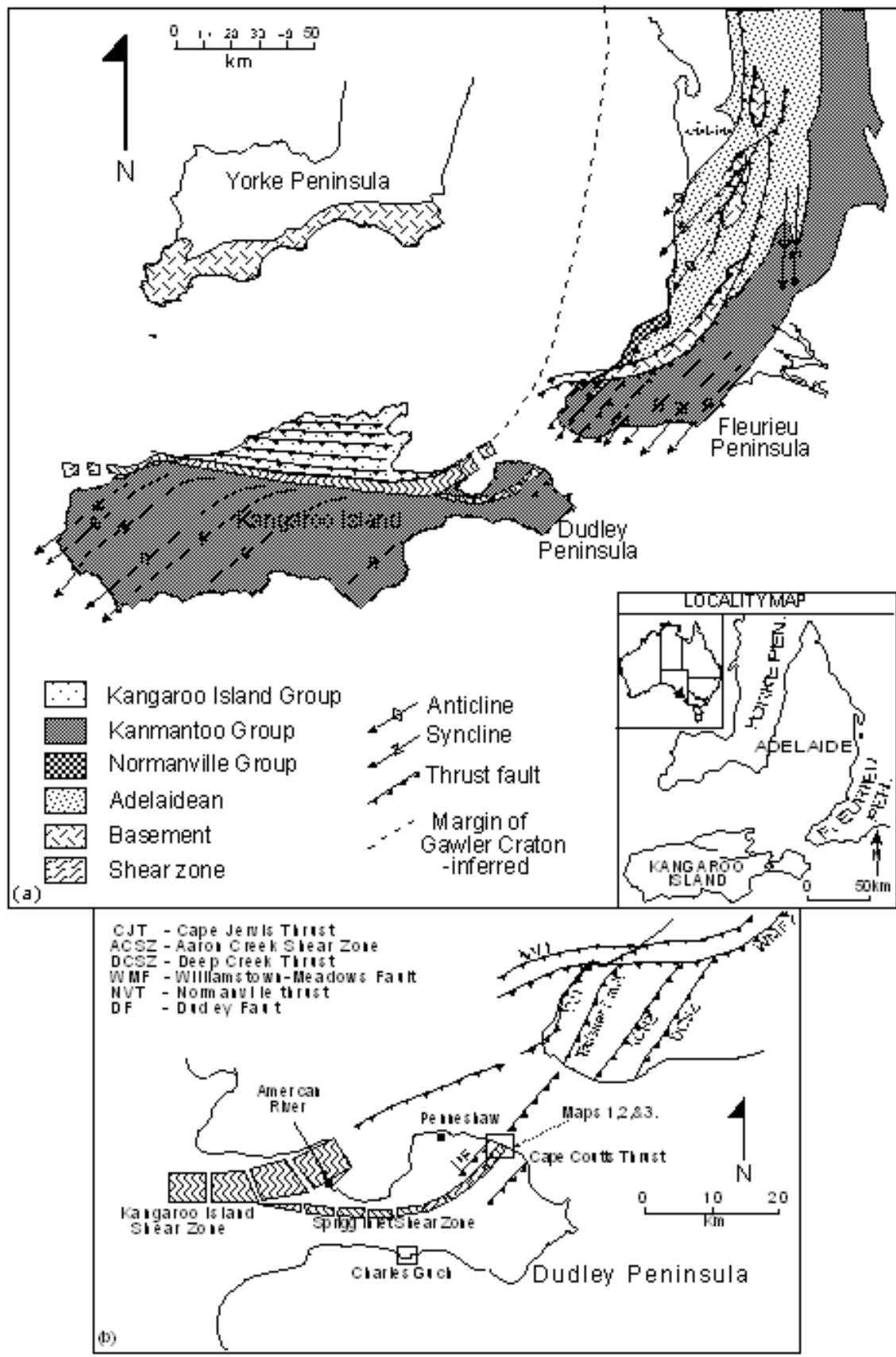


Fig.1 - (a) Principal geological features of the Southern Adelaide Fold-Thrust Belt. (b) Previous interpretation of the principal geological features on Dudley Peninsula and southern Fleurieu Peninsula. Note the curve of the Sprigg Inlet Shear Zone, connecting to the Kangaroo Island shear zone south of American River. Adapted from Flottmann and James 1997.



---

---

Bent fold belts can be classified into thick-skinned or thin-skinned origins, distinguishable by the involvement of substantial proportions of crust or the restriction to a thin upper crustal layer above a basal decollement.

Furthermore, bends can be classified as non-rotational 'arcs' or rotational 'oroclines'.

A non-rotational arc, as proposed by Marshak (1988), refers to bends in which the strike of segments within a bend does not change during formation of the orogen. An orocline refers to a bend in which the strike of segments within the orogen changes during deformation. Oroclines result from bending of an initially straight fold-thrust belt during a later deformation event. Oroclinal bends commonly result when a fold-thrust belt is moulded onto the corner of an irregularly shaped continental margin or other basement obstacle during the final stages of collision (Carey, 1955).

The Fleurieu arc is the southern most extension of the Adelaide Fold-Thrust Belt extending from Fleurieu Peninsula to Kangaroo Island. The formation of the arc or 'orocline' and its relationship to deformation has been the subject of considerable debate (Daily and Milnes, 1973; Clarke and Powell, 1989; Manktelow, 1990; Marshak and Flottmann, 1996; Flottmann and James, 1997). The results of these studies had led to two postulations of the Fleurieu Arc formation. These are;

- 1) The arc reflects the initial basin architecture of the Kanmantoo and Adelaidean basins. Cambro-Ordovician N-W directed shortening, reactivated down to basin curved growth faults in the underlying Gawler Craton. These former growth faults controlled the geometry of folds, thrusts, and shear zones within the fold belt (Flottmann and James, 1997).
- 2) Oroclinal bending of the fold-thrust belt was due to Cambro-Ordovician shortening being initiated and centred on the SE corner of the Gawler Craton (Marshak and Flottmann, 1996).

---

---

Alternatively, the true origin of the bend could be the result of a combination of components from both these two models.

The Dudley Peninsula lies within the apex of the Fleurieu Arc, making it an ideal location for testing the above stated models of formation of the Fleurieu Arc. On Dudley Peninsula, the structural grain has been interpreted previously (Flottmann and James, 1997) to bend through 50°, from NE-SW on the north coast, to E-W within the western part of the peninsula. The structural grain throughout Dudley peninsula was previously defined by the Sprigg Inlet Shear Zone (SISZ), which is a structurally complex, low-grade shear zone outcropping on the NE coast of Dudley Peninsula. Inland, the shear zone does not outcrop, yet has been interpreted in this study from magnetic data.

In this study, the SISZ and parts of the surrounding geology were mapped in detail, and structures recorded in order to gain a better understanding of the processes active during the Delamerian Orogeny. Specifically, to obtain a more sophisticated model for the development of the arcuate SAFTB (Marshak and Flottmann, 1996; Flottman and James, 1997).

## **1.2 Aims and methods**

The aim of this study was to describe and analyse some aspects of the structural geometry and evolution of the Dudley Peninsula paying particular attention to the SISZ.

The position of the Dudley Peninsula relative to the Gawler Craton (fig. 1a) makes this an ideal location for testing the stated theories of formation of the Fleurieu Arc. A structural appraisal of the area could yield new input into these theories, in particular:

- a) The structural and tectonic framework of the SISZ.
- b) The kinematic and strain history during deformation within the SISZ.

- 
- 
- c) The stress conditions of the SISZ and the tectonics of Dudley Peninsula in comparison to those on southern Fleurieu Peninsula and western Kangaroo Island.

A structural appraisal of the Dudley Peninsula was initiated by background research of previous studies of the SISZ, (Dailey and Milnes, 1971; Daily and Milnes, 1972; Menpes, 1992) and of the SAFTB (Offler and Flemming, 1968; Mancktelow, 1990; Jenkins and Sandiford, 1992; Flottmann et al. 1994; Marshak and Flottmann, 1996; Flottmann and James, 1997; Belperio et al. 1998). This led to the recognition of the need for a detailed structural interpretation of the NE coast of Dudley Peninsula, in particular the SISZ.

Field mapping of the NE coast of Dudley Peninsula determined the distribution of lithologies and minor structures. Measurements of minor structures included the orientation, shape, classification, and distribution of layering, veins, folds, foliations, lineations, and cleavages. Oriented hand specimens were collected for analysis of fold styles and vein geometries. Thin sections were made to analyse petrology and kinematic indicators.

Photographs and field sketches were made of veins, folds, faults, and boudins, which were used for classification, and strain analysis. Veins were analysed by stereographic projections. Folds and boudinaged layers were reconstructed to their pre-strained state in order to quantify strain.

An attempt was made to constrain the geographical limits of the SISZ, by coastal outcrop mapping on the southern coast of Dudley Peninsula, and by an interpretation of magnetic data from eastern Kangaroo Island. Structural features on the south coast of Dudley Peninsula were compared to the structural features observed on the NE coast. These comparisons were useful in interpreting the relative position of the SISZ to the mapped coastal outcrops, which was supported by the analysis of magnetic data.

---

---

## **2. GEOLOGICAL OVERVIEW**

### **2.1 Stratigraphy on Dudley Peninsula**

Coastal outcrops on Dudley Peninsula show turbidite flysch sequences of the Kanmantoo Group stratigraphically overlying rocks of the Normanville Group and sequences of the Adelaidean Supergroup. Adelaidean and Normanville Group lithologies outcrop on a 2 km long strip of coastal outcrop on the NE coast of Dudley Peninsula, surrounding Cuttlefish Bay.

The Cuttlefish Bay area has attracted much attention in the past (Daily and Milnes, 1971,1972,1973; Daily et al. 1979; Preiss,1987; Menpes, 1992) since it has the only outcrop of Adelaidean sediments on Kangaroo Island. These studies concentrated on the lithological interpretation of the Adelaidean and Normanville Groups, the interpretation of which is varied due to the deformed nature of the rocks, and to the remoteness from other Adelaidean and Normanville Group outcrops (e.g, on western Fleurieu Peninsula, and the Mt Lofty Ranges).

The stratigraphic nomenclatures used in this study have been adapted from those obtained from the Primary Industry and Resources of South Australia (PIRSA) Kanmantoo dataset.

### **2.2 Structure of the Fleurieu Arc**

The Dudley Peninsula lies within the syntaxial Fleurieu Arc (fig.1). This arc includes the Mount Lofty Ranges, the Fleurieu Peninsula, and Kangaroo Island. On Fleurieu Peninsula, regional structures include NW verging tight folds with wavelengths of 10 to 15 m, which parallel imbricate and basement involved thrusts and shear zones (Marshak and Flottmann, 1996).

West of Dudley Peninsula, the Kangaroo Island Shear Zone is the dominant regional structure. This shear zone strikes E-W from American River to Harveys Return. Directly north of the shear zone several imbricate thrusts

---

---

striking E-W, affect Cambrian platformal basin sediments of the Kangaroo Island Group (Flottmann and James, 1997). South of the shear zone, NW verging asymmetric open folds consisting of 4-8 km wavelength anticlines and 2-4 km wavelength synclines, extend to the western and southern coasts of Kangaroo Island (Marshak and Flottmann, 1996).

Interpretation of seismic reflection data beneath Backstairs Passage, shows a large number of listric, SE dipping planes of discontinuity, which merge into a basal reflector at 12-13 km depth (Flottmann and Cockshell, 1996). From this it is interpreted that the Kangaroo Island Shear Zone merges into a zone of imbricate thrusting below Backstairs passage, which is continuous onto southern Fleurieu Peninsula.

Previous studies have recognised the SISZ to be an eastern extension of the Kangaroo Island Shear Zone (Flottmann et al. 1995). The SISZ was assumed to have a regional arcuate nature in plan view, connecting to the Kangaroo Island Shear Zone south of American River (fig. 1b). To the north, the Cuttlefish Bay area was described as being structurally analogous to the Talisker area, on southern Fleurieu Peninsula (Flottmann et al. 1995).

### **2.3 Deformation of the SAFTB**

Kanmantoo and Adelaidean sediments of the SAFTB were subjected to a single orogenic event, the Delamerian Orogeny. Within this Cambro-Ordovician compressive orogeny, three phases of deformation (D1 – D3) have been recognised (Offler and Flemming, 1968).

Based on the observation that NE-trending faults truncate N-trending folds on western Fleurieu Peninsula, Offler and Flemming (1968) suggested this region was subjected to two deformation events. The first deformation (D1) event resulted in top to the west movement, and the second deformation (D2) resulted in top to the NW movement.

---

---

Alternatively, in the Southern Mt Lofty Ranges, Southern Fleurieu Peninsula, and on Kangaroo Island, the initial deformation (D1) is considered to be dominated by NW directed fold and thrust development. The intensity of D1 deformation decreases substantially from south to north with first generation thrusts dominant on Kangaroo Island and Fleurieu Peninsula (Belperio, 1998).

On Fleurieu Peninsula, D2 features include upright folds with N-S trending fold axes, and axial planar crenulation cleavages, which overprint first generation features (Belperio et al. 1998). On Kangaroo Island, there is evidence of multiple deformation events within the Kangaroo Island Shear Zone, and from fold interference patterns on western Kangaroo Island (Flint and Grady, 1979). However, it appears that the Fleurieu Arc developed during the initial NW-directed deformation phase (D1), prior to the onset of the E-W compressive deformation (D2) (Belperio et al. 1998).

### **3. GEOLOGY OF THE DUDLEY PENINSULA**

#### **3.1 Structural analysis of the NE coast of Dudley Peninsula**

Outcrop on Dudley Peninsula is restricted to coastal strips, with inland areas covered by Cenozoic aeolian dunes and clay rich lateritic soils. The area mapped (map1, map2, map3) lies between Snapper Point and Alex Lookout on the NE coast of Dudley Peninsula. Outcrops are displayed in cliff and wavecut platform exposures of Kanmantoo Group, Normanville Group, and Adelaidean Supergroup metasediments.

The youngest outcropping metasediments of the Kanmantoo Group (i.e. Talisker-Calc siltstone) occur in the limits of the area mapped (map1). From the SE, outcrops of metasediments are progressively older towards the core a major fold, termed the Cuttlefish Bay Anticline (CBA). The oldest metasediments in the mapped area are of the Sturt Tillite which occurs within the core of the CBA, outcropping ~200 m north of Cuttlefish Bay.

---

---

The metasediments in the area mapped strike consistently between 030° to 050° and dip moderately (40°-70°) towards the SE. Graded bedding within pelitic units indicates these rocks are right way up in the SE limb, and overturned within the NW limb of the CBA.

Four structurally distinct domains were chosen in the mapped area for detailed structural interpretation and analysis. These domains were chosen to represent the variations in strain accommodation and styles of deformation observed within the area mapped. These domains are;

(1) - The Cuttlefish Bay Anticline (Domain 1 – CBA) is a major fold showing deformation features indicative of intense strain within the core of the fold.

(2) - The Sprigg Inlet Shear Zone (Domain 2 – SISZ) is exposed for 800 m in and around Sprigg Inlet. The shear zone is developed within the southern upright limb of the CBA, within interbedded metasandstone and phyllites of the Normanville Group. This shear zone is characterised by LS tectonite fabrics within andalusite and staurolite bearing metapelites, and garnet bearing metapsammities. The SISZ is given particular attention in this study as it displays key structural relationships that have implications for the wider tectonic development of the Fleurieu arc.

(3) - The Snapper Point Homoclinal Zone (Domain 3 – SPHZ), directly SE of the SISZ, contains small-scale buckle folds. The fold axes of these folds show a progressive change in orientation with respect to the distance away from the SISZ.

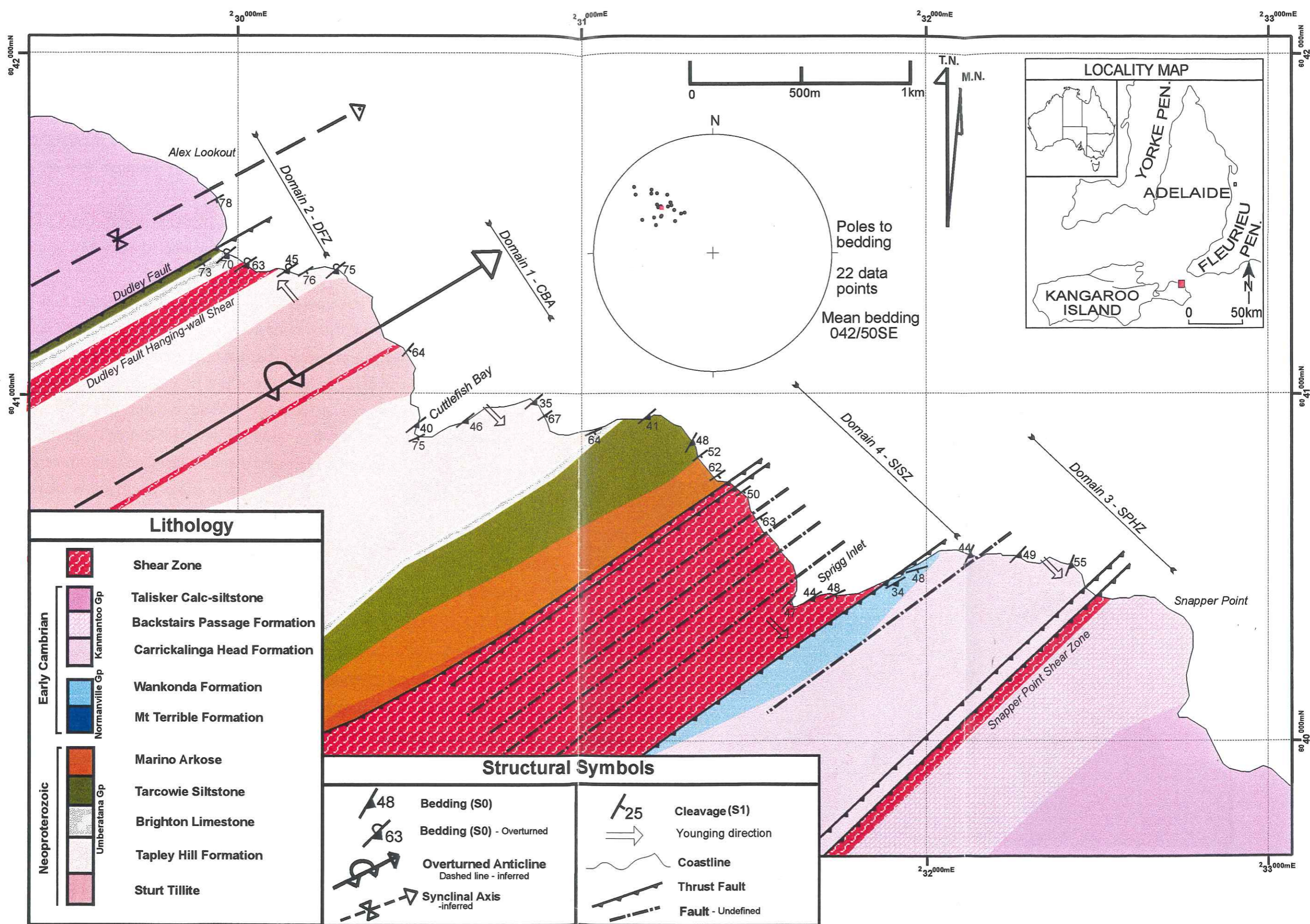
(4) – The Dudley Fault Zone (Domain 4 – Dudley Fault Zone (DFZ) is characterised by intense folding and shearing developed around the Dudley Fault. The Dudley Fault is developed on the NW overturned limb of the CBA, and shows structural features indicating intense strain within the fault zone. A major stratigraphic offset occurs at the Dudley Fault, with Neoproterozoic age

---

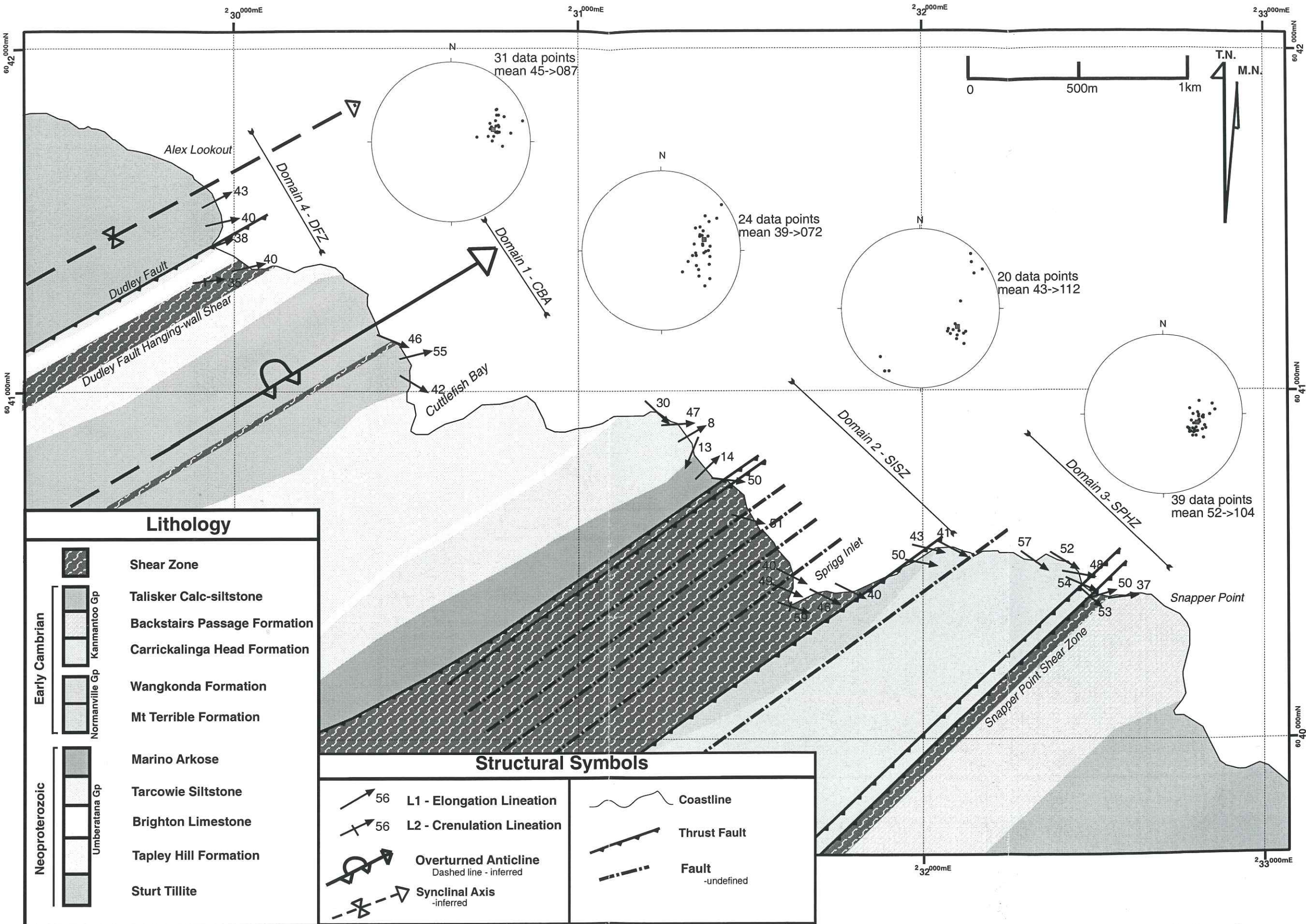
---

metasediments of the Tarcowie Siltstone in the hangingwall, juxtaposed against Early Cambrian age rocks of the Talisker Calc-siltstone in the footwall.

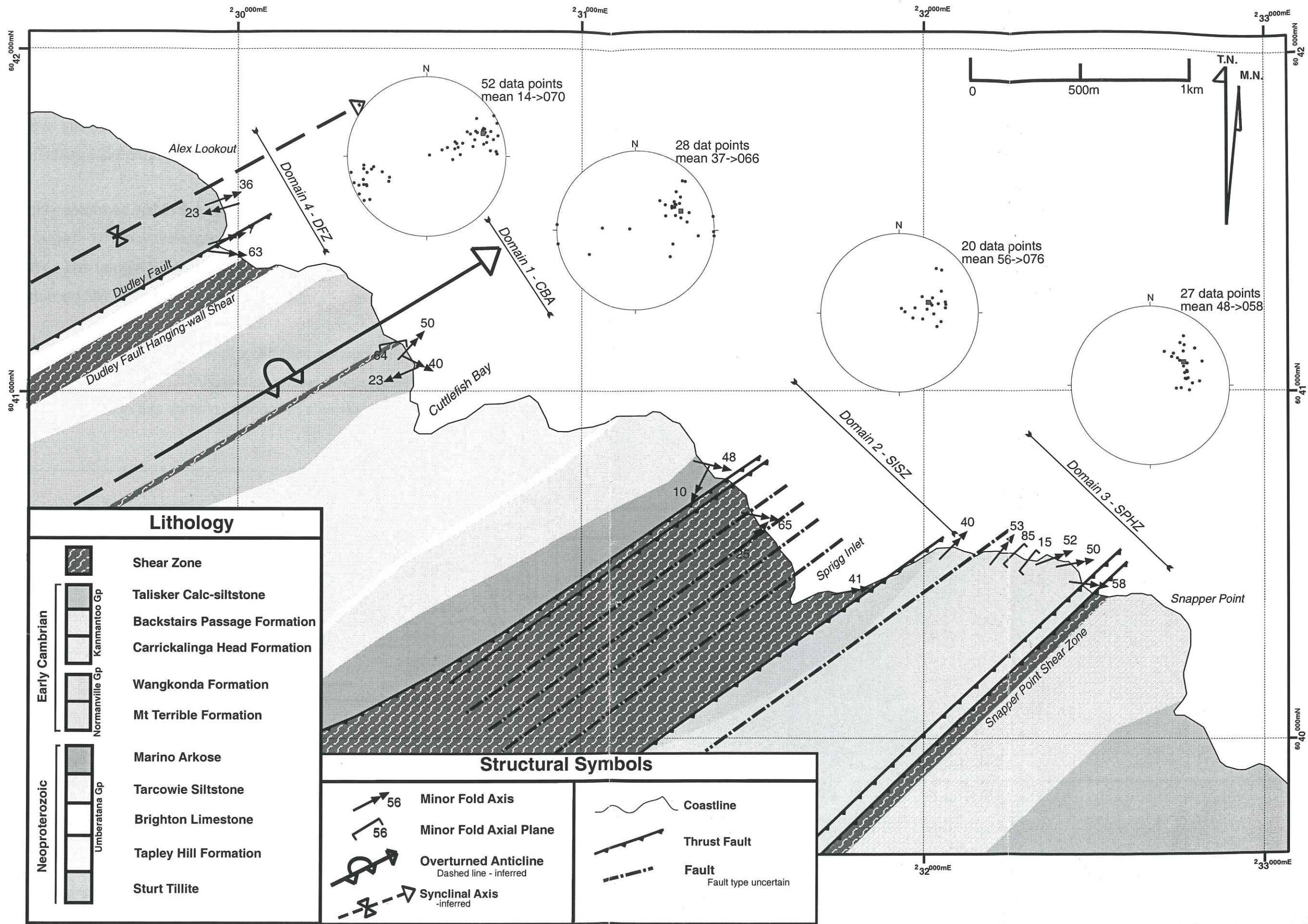




**Map 1 - Lithological and structural interpretation of coastal outcrop on NE Dudley Peninsula, Kangaroo Island. Bedding and cleavage measurements.** Inset shows location of mapped area. Lower hemisphere stereographic projection shows regional pole to bedding measurements. Mean of poles to bedding shown by red square.



**Map 2 - Lithological and structural interpretation of coastal outcrop on NE Dudley Peninsula, Kangaroo Island. Mineral lineation data.** Lower hemisphere stereographic projections show mineral lineation measurements from each of the four domains. Mean lineation orientation shown by red square.



**Map 3 - Lithological and structural interpretation of coastal outcrop on NE Dudley Peninsula, Kangaroo Island. Fold axis and fold axial plane orientations.** Lower hemisphere stereographic projections show fold axis orientation data from each of the four domains. Mean fold axis orientation within each domain shown by red square in stereonet.

---

---

### 3.1.1 Domain 1 – The Cuttlefish Bay Anticline (CBA)

The Cuttlefish Bay Anticline is, because of its size and structural significance, the most pronounced fold outcropping on the coastline of Dudley Peninsula. Rock units within this domain consist of the Sturt Tillite, within the core of the CBA, and the Tapley Hill Formation, which outcrops at Cuttlefish Bay.

Bedding is highly deformed within the core of the tight Cuttlefish Bay Anticline. The CBA is a large (~10 km wavelength), overturned fold, which verges towards the NW. The upright SE limb of the CBA has a moderate (~40°) dip, while the overturned NW limb has a steep (~65°) dip.

A 50 m cross section sketch was drawn of a cliff-face outcrop ~50 m south of the axial plane of the CBA (fig. 2). This section shows a representation of the large variety of fold styles in this domain, along with a series of faults spaced 5 to 10 m apart.

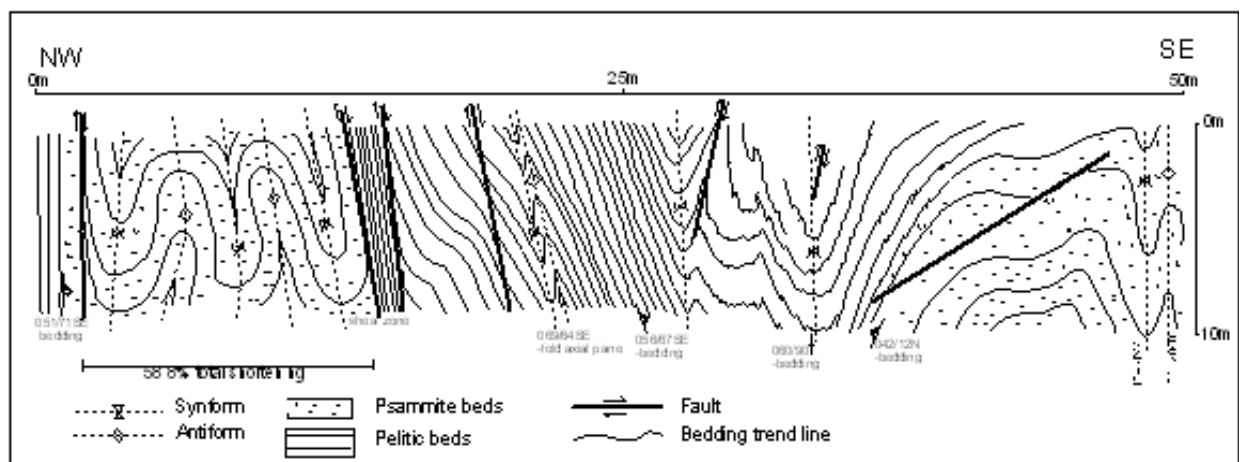


Fig. 2 – Sketch of vertical cliff exposure 200 m north of Cuttlefish Bay. The axial plane of the CBA is presumed to be 50 m to the NW from the zero meter mark of this sketch. This sketch was drawn as if looking from the SW towards the NE.

The faults observed in this section dip steeply (~80°) towards both the SE and NW. Movement on all these faults as defined by the drag of bedding into the fault plane, is downthrow of the SE block, indicating both high angle reverse

---

---

and normal movement. There is an absence of quartz veining and an absence of brittle fault rocks near the fault planes.

Parasitic folds within psammite layers in the NW part of this section (fig. 2), are tight to isoclinal, round, upright, flattened class 1C folds (Ramsay and Huber, 1987). Parasitic folds developed in pelitic layers, vary from tight folds with angular fold hinges, to round, close folds with small-scale folds (~5 cm wavelength) developed within the fold hinges.

The SE part of this section shows folded psammite layers where the fold axial plane is sub-parallel to the cliff-face section, hence this gives a false indication of the true fold style. Folds in this domain dominantly have a gentle to moderate plunge (30°-50°) towards the NE, with steeply inclined (64°) to upright (90°) fold axial planes. However, there are variations of fold axis orientation within this domain (see stereogram from Map 3), which include folds with a moderate plunge (30°) towards the SE, and a few fold axes which plunge towards the W to SW with gentle (25°) to sub-vertical (85°) plunges.

Thin (0.5 – 2 cm) planar tension gash veins of massive quartz, occasionally occur within the axial planar cleavage of the minor parasitic buckle folds described above. Also in this domain, abundant syn-kinematic garnet porphyroblasts up to 4 mm in diameter occur within psammites and in close proximity (within 2-5 cm) to quartz veins. These porphyroblasts show a sigmoidal internal fabric, and display asymmetric strain shadows comprising of biotite and quartz which resemble  $\delta$ -type and  $\sigma$ -type geometries (Passchier and Simpson, 1986), showing SE over NW bulk shear sense. There is also a widespread overgrowth of post-deformational scapolite.

### **3.1.2 Domain 2 – The Sprigg Inlet Shear Zone (SISZ)**

The Sprigg Inlet Shear Zone outcrops on an 800 m wide coastal section in and around Sprigg Inlet. The outcrop consists of andalusite/staurolite bearing LS tectonites, with abundant quartz veins, folds, faults and boudins.

---

---

The shear zone is developed within the Normanville Group metasediments of the Wangkonda Formation and the Mt Terrible Formation. These sediments dominantly comprise of phyllitic beds, from ~1 cm to 2 m thick, occasionally interbedded with quartzite layers up to 50 cm thick. Phyllitic layers often show graded bedding which defines a younging direction within the shear zone. The younging direction is consistent towards the SE. Bedding is also consistent in orientation throughout the shear zone striking ~045° with a moderate (~45°) dip to the SE. A lineation defined by the preferred orientation of biotite is consistent throughout the shear zone, plunging 50° towards the SE (120°).

Lineations within shear zones generally develop parallel to the shear direction (McClay, 1997). However, lineations do not ideally record the principal displacement vector. More specifically, lineations are developed in response to the strain distribution during mineral growth, and may reflect variations in along-strike strain, and/or strain partitioning (Tikoff and Greene, 1997). There is a definite difference in strain features observed in sections perpendicular to the SISZ. Hence, it is necessary to specify the orientation of these sections in relation to the local finite strain ellipsoid. In the case of this study, the main transport direction is assumed to lie parallel to the lineation direction defining the X direction of the local finite strain ellipsoid (fig. 3a). The Y direction is assumed to be sub-horizontal, striking along the bedding planes, with the Z direction perpendicular to the layer parallel to sub-parallel foliation developed within fine-grained pelitic units throughout the shear zone.

Wave-cut platforms within the SISZ cut across bedding, and show structural features that represent the YZ (low strain) plane of the local finite strain ellipsoid. Cliff sections within the SISZ are developed sub-parallel to the lineation direction, and perpendicular to the strike of bedding, thereby exposing structural features representing the XZ (high strain) plane of the local finite strain ellipsoid (fig. 3b).

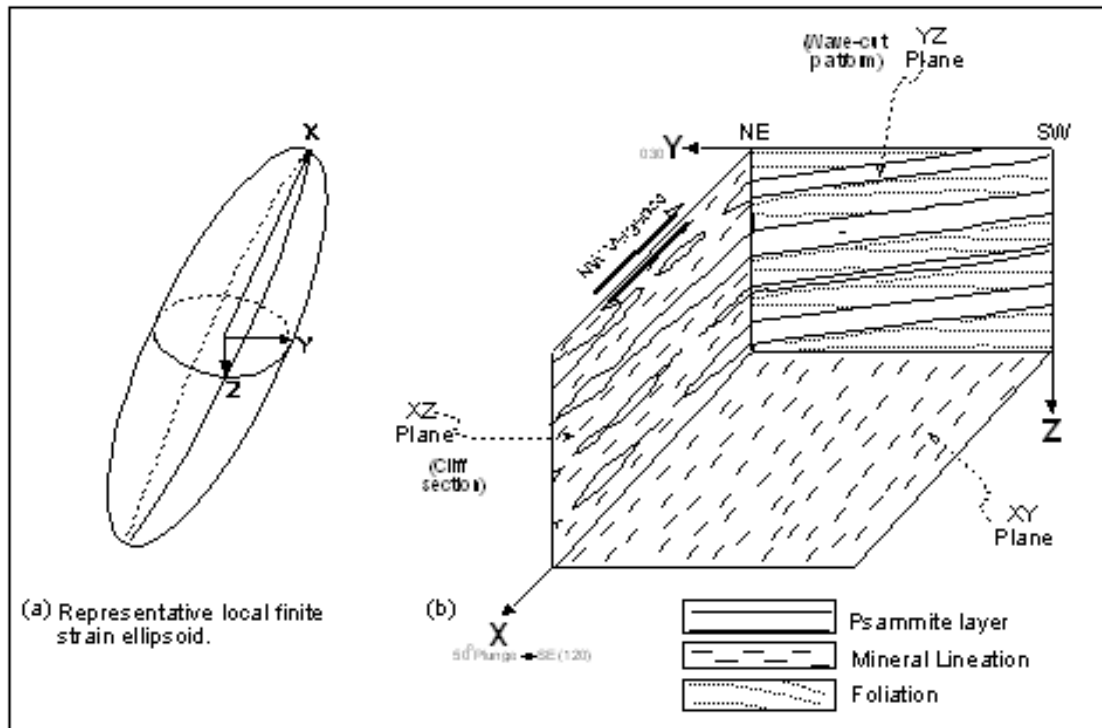


Fig. 3 – Cartoons showing (a) the orientation of the representative finite strain ellipsoid within the SISZ, and (b) the orientation of the XZ (high strain), XY (foliation), and YZ (low strain) planes within a representative 3-D block from the SISZ. Representative structural features are shown on each plane with, the mineral lineation shown on the XY plane, shearband-type boudins on the XZ plane, and a refracted foliation on the YZ plane (note, the foliation is developed within pelitic units, and is refracted from layer parallel to oblique to bedding). Perspective view drawn looking from NW towards the SE, up and underneath main foliation (XY). Unusual view drawn as this is the form of many upstanding coastal outcrops.

Within the SISZ there is a well-developed slaty cleavage (S1), which penetrates pelitic layers. Between Sprigg Inlet and the northern boundary of the shear zone this foliation is dominantly layer parallel. Whereas, at a location 50 m east of Sprigg Inlet there is a distinctive pattern of refracted cleavage within pelitic units (fig. 4b).

At this location there are two foliations within pelitic beds, as observed on the YZ plane. The dominant foliation is refracted from layer parallel, to dip moderately ( $\sim 45^\circ$ ) towards the NE in coarser metasediments of pelitic beds. A weak foliation (just visible in the field) with a moderate ( $\sim 45^\circ$ ) dip towards

---

---

the SW is overprinted by the strong foliation. This weak foliation is also refracted into layer parallel in finer metasediments of pelitic beds (fig. 4b).

Overprinting criteria is observed in thin section with the development of a crenulation cleavage perpendicular to the layer parallel foliation. The layer parallel foliation is folded to form asymmetric folds with wavelength from 3mm (fig. 5a) to 1mm (fig. 5b). The crenulation lineation (L2) defined by the fold axis of the micro-folds is sub-parallel to the mineral lineation (L1). This crenulation was observed within Sprigg Inlet and at a location 200 m north of Sprigg Inlet. Otherwise the crenulation was not readily identified throughout the shear zone.

Abundant within the SISZ are andalusite porphyroblasts developed within fine metasediments of pelitic beds. These porphyroblasts are large (up to 2 cm in diameter), with asymmetric strain shadows comprising of biotite and quartz which show  $\delta$ -type and  $\sigma$ -type geometries (Passchier and Simpson, 1986), implying SE over NW movement. These winged porphyroblasts were observed in the field from cliff sections (XZ plane) and in thin section (fig. 6). In thin section, a curved internal fabric is observed within andalusite, staurolite, and garnet porphyroblasts, which also indicates SE over NW movement. Some porphyroblasts document relative rotation of more than 90° to the foliation.



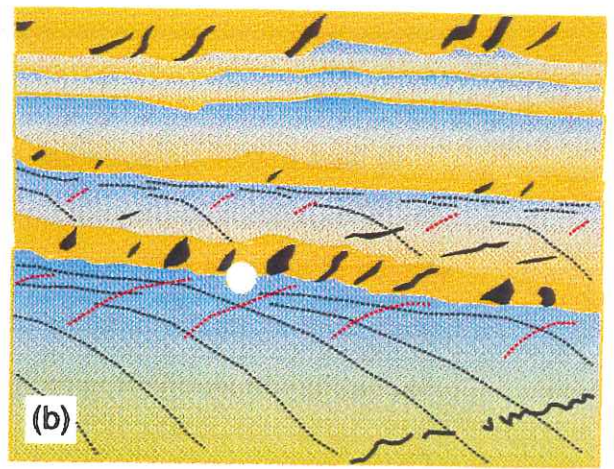
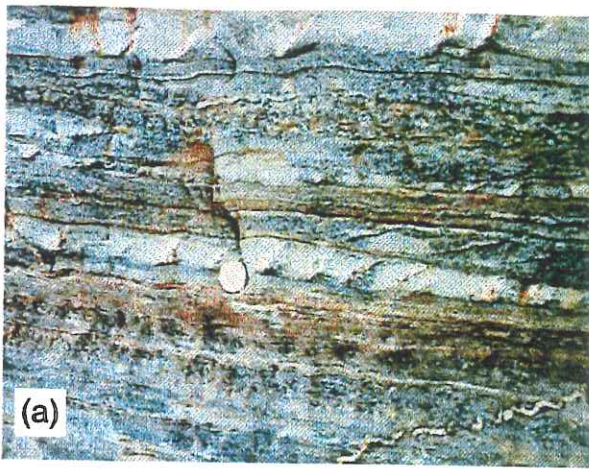


Fig. 4 - (a) Photo of interbedded metapelites and metapsammities from a location 50m east of Sprigg Inlet. Note the dominant set of sinistral veins within the central metapsammite unit. Photo looking SE. (b) Cartoon representation of features from photo(a), showing graded bedding from sandy (yellow) to silty (blue) sediments. Note the dominant foliation (black dotted line) within pelitic units, overprinting a weaker foliation (red dotted line). Both foliations are refracted.

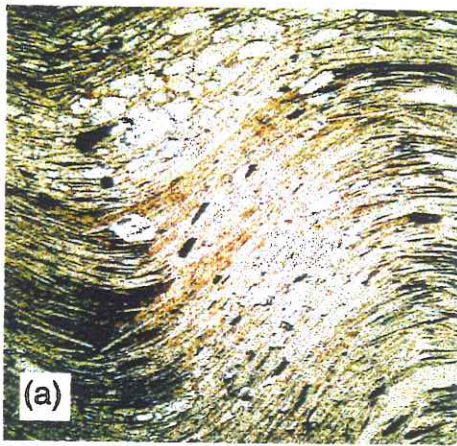


Fig. 5 - Thin section photos showing asymmetrically micro-folded slaty cleavage with wavelengths of (a) 3 mm and (b) 1 mm, developed within biotite rich metapelitic unit 200 m north of Sprigg Inlet, within the SISZ. Plane polarized light. Field of view is 4mm.

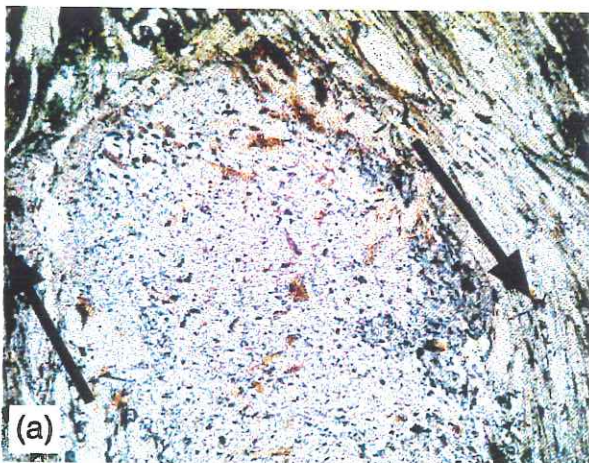


Fig. 6- (a) Thin section photo and (b) cartoon representation of staurolite(yellow) replacing andalusite (purple). Not evident in the photo is an internal fabric within the porphyroblasts which shows relative rotation of the porphyroblast to the external fabric. Quartz grains (blue in (b)) are elongated within the quartz/biotite matrix. Antithetic micro-shear shown by dotted line. Large biotite crystals (green in (b)) are present within strain shadow. Field of view is 4mm. Sprigg Inlet Shear Zone.

---

---

Quartzite layers within a cliff section (XZ plane) outcropping 150 m east of Sprigg Inlet display shearband-type boudins (fig. 8b), with individual boudins consistently rotated slightly ( $\sim 2^\circ$ ) towards the foliation. The foliation is slightly oblique ( $\sim 5^\circ$  steeper angle) to bedding. Winged porphyroblasts of andalusite are aligned parallel to this foliation indicating SE over NW bulk shear sense.

Boudins are also observed on the YZ plane throughout the shear zone. Twenty meters inside the southern boundary of the SISZ, psammite units are up to 40 cm thick. Here, the thick psammite units show drawn boudins and ramp-folded structures (Goscombe and Passchier, in prep.) (fig. 7a, fig. 8a). The boudins are partly folded, and rotated, with the majority of boudins rotated clockwise (as viewed from above), and a minority of boudins rotated anti-clockwise (as viewed from above). Sigmoidal veins comprising of massive quartz occur between individual boudins. Two opposing geometries of the sigmoidal interboudin veins are observed, which resemble the letters S and Z (fig. 7a). Pelitic beds and thin (<1 cm thick) psammitic units envelope the thick quartzite boudins, which show consistent asymmetric overfolds verging towards the NE. Within thick (30 cm) pelitic units, foliation boudinage is observed on the YZ plane, as shown at a location 100 m east of Sprigg Inlet (fig. 7b).

# Array of structures within the Sprigg Inlet Shear Zone.

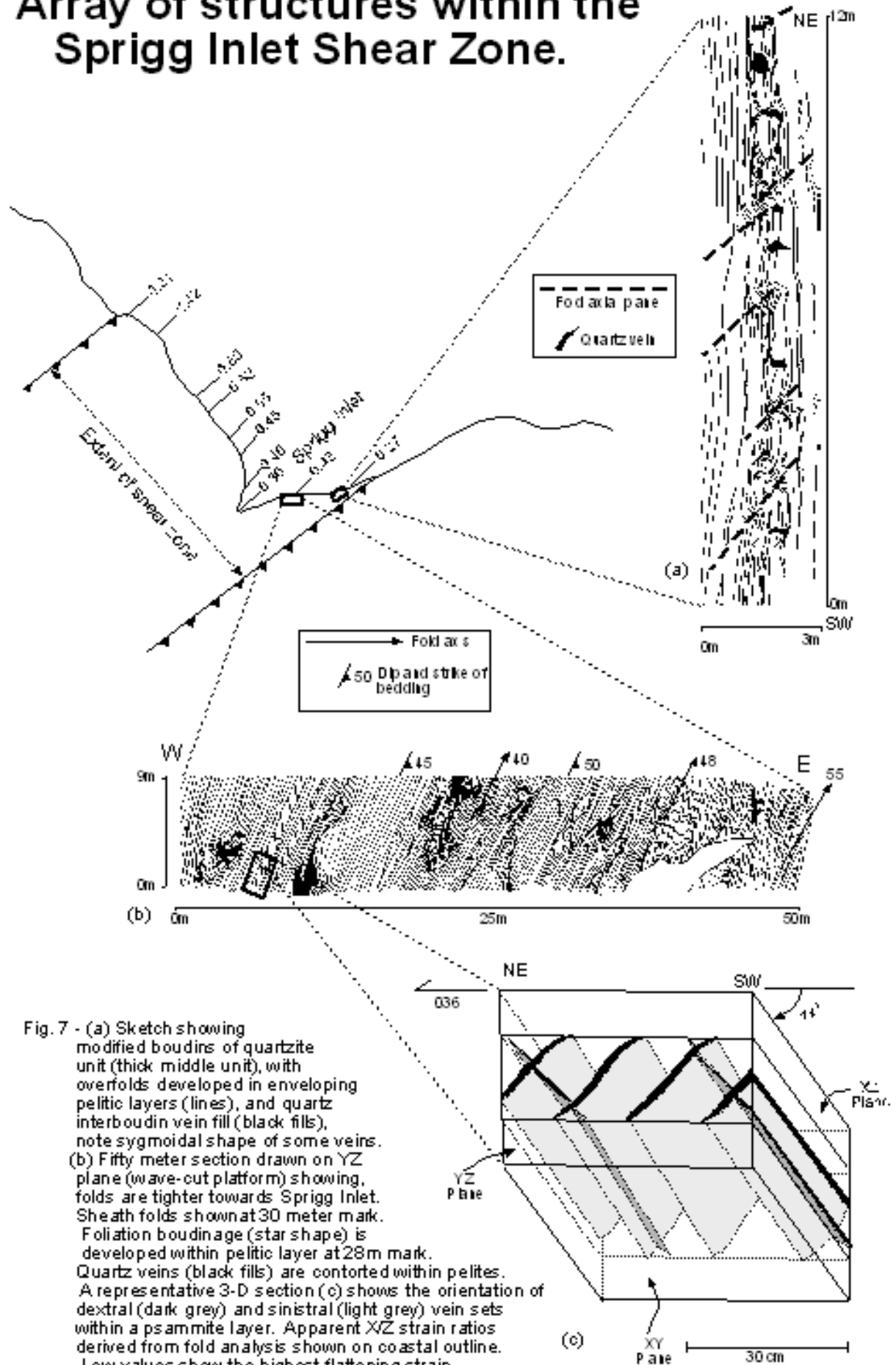


Fig. 7 - (a) Sketch showing modified boudins of quartzite unit (thick middle unit), with overfolds developed in enveloping pelitic layers (lines), and quartz interboudin vein fill (black fills), note sigmoidal shape of some veins.

(b) Fifty meter section drawn on YZ plane (wave-cut platform) showing folds are tighter towards Sprigg Inlet. Sheath folds shown at 30 meter mark.

Foliation boudinage (star shape) is developed within pelitic layer at 28m mark.

Quartz veins (black fills) are contorted within pelites.

A representative 3-D section (c) shows the orientation of dextral (dark grey) and sinistral (light grey) vein sets within a psammite layer. Apparent X/Z strain ratios derived from fold analysis shown on coastal outline.

Low values show the highest flattening strain.

---

---

Within psammite units, at a location 50 m east of Sprigg Inlet, there is a set of deformed planar and occasionally sygmoidal *en-echelon* tension gash veins comprising of massive quartz. The extent of the veins is restricted within the width of the psammite units. The veins are generally 1 to 2 cm wide and are evenly spaced about 10 cm apart. These veins have a consistent orientation throughout the shear zone striking N-S, and have a steep 75°E dip. It is presumed that this vein set formed during sinistral strike-slip movement within the SISZ, thereby these are defined as the sinistral vein set (for further discussion see chapter 4.2). In pelitic units, quartz veins up to 2 cm thick are generally much longer in length (up to 1m) and often have a gentle dip. Most quartz veins within pelitic units are folded, with fold wavelengths of about 2 to 5 cm and amplitudes of 1 to 10 cm. The fold axes of the folded quartz veins are often aligned with the preferred orientation of biotite within the shear zone.

At a location 100 m east of Sprigg Inlet, two sets of quartz veins are developed within a psammite unit (fig. 7c). The prominent sinistral set of *en-echelon* quartz veins as described above, offsets a much less prominent set of planar and occasionally sygmoidal *en-echelon* tension gash veins of massive quartz. The less prominent vein set strikes E-W, and has a moderately 45°S dip. For the sake of definition this vein set is defined as dextral, as is assumed to have formed during dextral strike-slip movement within the SISZ. The dextral veins are thin (1mm to 1cm), and do not have a regular spacing.

The dextral sets of veins are much less abundant than the sinistral veins, the latter of which occurs throughout the SISZ. However, in every case the sinistral set of veins crosscut and offsets the dextral veins (fig. 9). North of Sprigg Inlet there is a greater abundance of layer parallel massive planar quartz veins, with crosscutting veins less abundant.

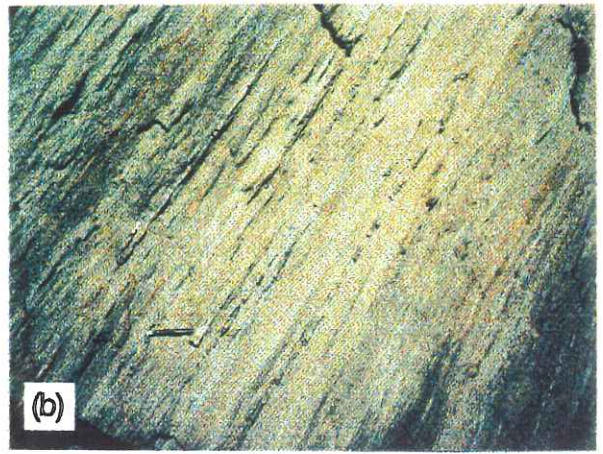
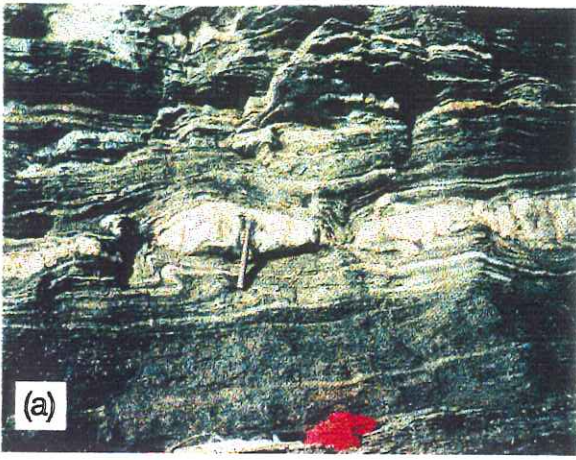


Fig. 8 - (a) Ramp-folded structure developed within XY section 180 m east of Sprigg Inlet. Photo looking SE. (b) Shearband-type boudins developed within thin (~5 cm thick) quartzite layers, as observed within a cliff face 150 m east of Sprigg inlet. Photo looking SW. Sprigg Inlet Shear Zone.

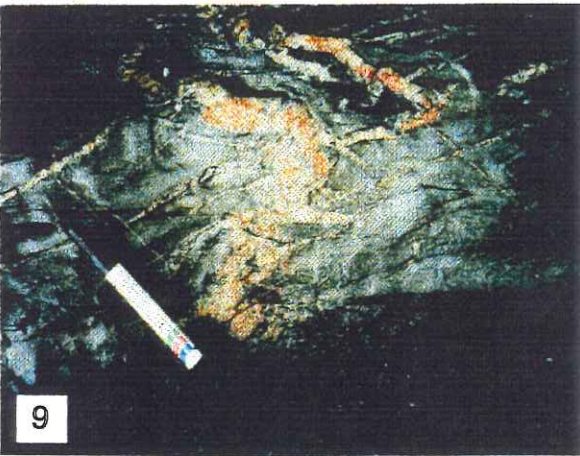


Fig. 9- Photo showing vein types within a metapsammite unit from a location 75 m east of Sprigg Inlet. Thick central quartz vein is sygmoidal interboudin vein. Note thin sinistral veins crosscut and offset less abundant dextral veins (parallel to marking pen). Photo looking SE.

Fig. 10- Photo showing highly contorted chlorite rich quartzite layer within massive metapelite, 5m SE of the SE boundary of the SISZ. Note double plunging fold in upper left of photo. Photo looking SE. Field of view 5 m.

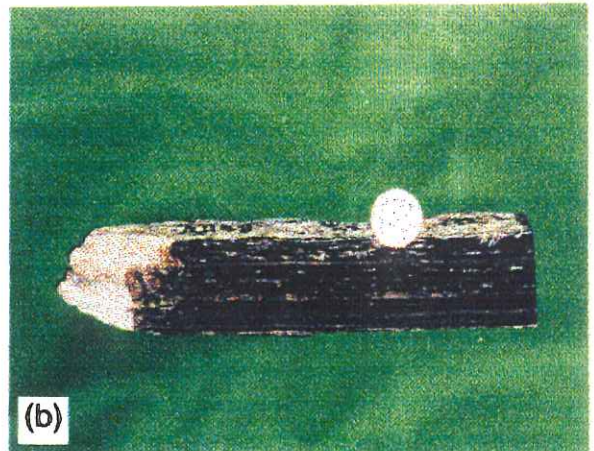
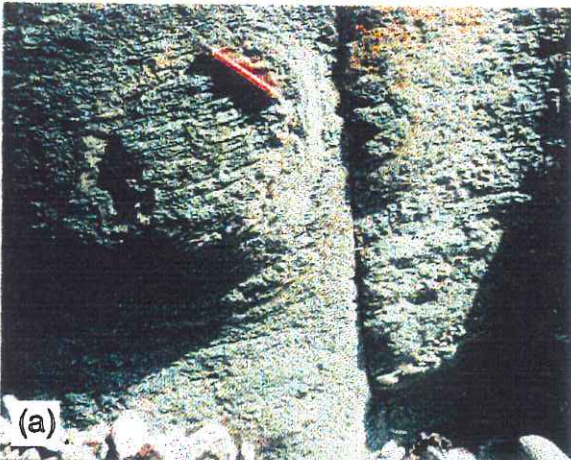


Fig. 11- (a) Photo of actinolite/cordierite rich hornfels at the northern boundary of the SISZ. Note the sub-horizontal lineation. Photo looking NW. (b) Photo of laminated hornfels hand specimen from northern boundary of the SISZ. Coin is 25 mm wide.

---

---

There is a wide array of fold types developed within the SISZ. The majority of folds are harmonic, class 1C (Ramsay and Huber, 1987), tight to isoclinal, gently inclined ( $20^\circ$ ) folds with a mean moderate plunge ( $43^\circ$ ) towards the east ( $112^\circ$ ). Also in this domain, there are a few folds with upright to steeply inclined (to the SW) fold axial planes with fold axes that plunge gently ( $25^\circ$ ) towards the NE (see stereogram from map 2).

Non-cylindrical folds occur at a few locations within and surrounding the SISZ. A wavecut platform section, located 100 m east of Sprigg Inlet (fig. 7b), shows a progressive change in fold style. The SE part of the section shows tight asymmetric folds, whereas the central part of the section displays isoclinal and non-cylindrical sheath folds.

The southern boundary of the SISZ is defined by a marked change in strain features with an obvious change in strain over a centimetre scale. A folded grey pelite is in contact with a flattened interbedded sand and siltstone, with intensely thinned layering. Five meters south of the shear zone boundary a chlorite rich quartzite layer is highly contorted, displaying tight to isoclinal and in part sheath folds (fig. 10).

The northern boundary of the shear zone is an intensely deformed, 40m wide fault zone. At the northern margin of the fault zone, in contact with relatively undeformed Marino Arkose, is a laminated cordierite, actinolite rich hornfels (fig. 11). The hornfels shows 2 to 3 mm thick laminations of alternating cordierite and hornblende layers, which dip to the SW, parallel with bedding in the area. The actinolite crystals are aligned sub-horizontally defining a lineation at  $90^\circ$  to those developed within the shear zone (Map 2).

A number of faults with SE dip occur north of Sprigg Inlet. These faults dip at various angles, from near vertical, to  $45^\circ$ , with smaller branches developed from the main fault plane dipping less than  $45^\circ$ . These faults show no evidence of sense of displacement.

---

---

North of Sprigg Inlet, large andalusite porphyroblasts (<3 cm diameter) are associated with minor staurolite. Also, north of Sprigg Inlet there are abundant garnets within psammites and within 1-2 cm halos around quartz veins, with post-kinematic scapolite more widespread.

### **3.1.3 Domain 3 – Snapper Point Homoclinal Zone (SPZ)**

The Snapper Point Homoclinal Zone is characterised by small-scale disharmonic folding of meta-sandstone, and fine (1 mm) biotite rich interbeds, of the Carrickalinga Head Formation. At Snapper Point, massive meta-sandstone units with very fine (~0.5 mm) biotite and heavy mineral laminations of the Backstairs Passage Formation, show modified boudins. A 20 m wide shear zone (the Snapper Point Shear Zone) is developed within a pelitic unit between these lithologies.

Within the Carrickalinga Head Formation disharmonic folds have a mean fold axis plunging 48° to the NE (058°). At a location 50 m SE of the southern boundary of the SISZ the disharmonic folds dominantly strike NE-SW, whereas towards the Snapper Point Shear Zone these folds progressively strike more towards the east (Map 2). The folds tend to align towards the lineation as defined by the preferred orientation of biotite closer to the Snapper Point Shear Zone.

There are abundant massive quartz and calcite veins within the Carrickalinga Head Formation in various orientations. Planar E-W striking dextral veins with a steep ~85°S dip are generally long (<2 m) and thin (~2 cm). Occasionally these veins are offset (up to 10 cm) by sinistral, planar, massive quartz and calcite veins, which are short (<15 cm) and thin (<2 cm). Within the Snapper Point Shear Zone, massive quartz and calcite veins (generally <2 cm thick) are intensely folded, with the fold axes aligned sub-parallel to the preferred orientation of biotite within the shear zone. Outside of the shear zone, veins are less intensely folded. Veins 100 m NW of the Snapper Point Shear Zone

---

---

are undeformed. The thickness and abundance of quartz veins also decreases NW of the Snapper point shear zone, however increases in abundance within 50 m of the SISZ.

Metapsammities of the Backstairs Passage Formation outcropping at Snapper Point display bone-type structures (Goscombe and Passchier, in prep.). Bone-type structures are developed by an original layer parallel torn component of boudinage orthogonal to a later flattening component of deformation (Goscombe and Passchier, in prep.). Sigmoidal interboudin veins comprising of massive quartz and calcite occur between individual boudins. The interboudin veins are generally thick (5-15 cm), upright to steeply inclined, and strike consistently between 100° to 120°.

Within the Snapper Point Shear Zone, retrogressed porphyroblasts of andalusite are highly flattened, defining an elongation lineation parallel to the preferred orientation of biotite. These porphyroblasts formed pre-deformational to syn-deformational with retrogression to quartz and biotite post-dating the foliation generation. The majority of the porphyroblasts are not suitable as kinematic indicators due to flattening of the porphyroblasts and a strong overgrowth of randomly orientated biotite. However, a few porphyroblasts show winged asymmetric features, which indicate east over west shear sense.

The northern boundary of the Snapper Point Shear Zone is a fault zone, 4-5 m wide, displaying isoclinal folds of 10 to 15 cm wavelengths, with the fold axial plane parallel to bedding, and a crenulation lineation plunging (53°) towards the SE. There is also an overgrowth of randomly orientated scapolite.

Two high angle faults intersect within this domain, one 30 m north of the Snapper Point Shear Zone, and an undifferentiated, near vertical, two-meter



---

---

wide fault zone which outcrops 500 m east (along the coastline) of Sprigg Inlet.

#### **3.1.4 Domain 4 – Dudley Fault Zone (DFZ)**

The Dudley Fault Zone displays structural features representing high strain. The most intense strain is recognised by isoclinal and sheath folds within a 2 to 3 m wide fault zone, termed the Dudley Fault. This is a NE striking thrust fault, steeply dipping ( $\sim 70^\circ$ ) to the SE. The fault surface displays an oblique lineation, defined by the preferred orientation of biotite, plunging  $40^\circ$  towards the NW. This fault displays significant stratigraphic offset, juxtaposing the Tarcowie Siltstone of the Adelaidean Supergroup in the hangingwall, from the Talisker Calc-siltstone of the Kanmantoo Group in the footwall.

The footwall metasediments display sheath folds within 50 m of the fault zone, with folds becoming more open away from the fault. The sheath folds are flattened perpendicular to their fold axial planes, which strike NE to SW and have a steep  $75^\circ$ SE dip. Within the fold hinges of these folds, small scale folds with  $\sim 5$  cm wavelength and  $\sim 3$  cm amplitude are developed parallel to the axial plane of the host folds.

Further north ( $\sim 75$  m) from the Dudley Fault, tight to close buckle folds are displayed. A change in vergence of these buckle folds defines a synclinal axis 100 m north of the Dudley Fault (Map 1).

South of the Dudley Fault, fold style and orientation change depending upon the distance from the fault zone. Within 10 m of the fault zone, there are isoclinal folds with NE to NNE striking fold axial planes, and fold axes which plunge gently to the NE. At one location 50 m south of the Dudley Fault, tight folds are displayed with axial planes striking E-W, and fold axes that plunge  $63^\circ$ E.

---

---

A shear zone is developed within a pelitic unit of the Tapleys Hill Formation 70 m south of the Dudley Fault, referred to here as the Dudley Fault Hanging Wall Shear. This 80 m wide shear zone is characterised by intense quartz veins up to 30 cm thick, and abundant andalusite porphyroblasts up to 3 cm in diameter. The winged porphyroblasts commonly display  $\delta$ -type and  $\sigma$ -type geometries (Passchier and Simpson, 1986) which indicate SE over NW shear sense. An internal fabric is present within the porphyroblasts, defined by quartz inclusions, which shows relative rotation of the porphyroblasts consistent with SE over NW movement. The porphyroblasts are elongated, with the elongation direction parallel to the preferred orientation of biotite within the shear zone, which dips 40°ENE. Also within the shear zone, a weak crenulation cleavage with a crenulation lineation (L2) parallel to the mineral lineation (L1), is exposed in an outcrop above the cliff top.

Within the shear zone, up to 30 cm thick quartz veins are highly contorted. Thin (<1 cm) veins are tightly folded, with the fold axial traces aligned with the preferred orientation of biotite within the shear zone.

Tension gash veins are preserved within 15 cm thick quartzite beds, 10 m south of the Dudley Fault Hanging Wall Shear. These veins are in 2 distinct orientations, one set of N-S (020°) striking, planar tension gash veins which dip (60°) towards the east, and a set of vertical, E-W (095°) striking tension gash veins.

Within the Talisker Calc-Siltstone, 5 m north of the Dudley Fault, there are abundant thin (1 to 5 mm) calcic veins. These veins cross cut the folded calc-siltstone, with some of these veins being thinned and boudinaged, while others are straight and undeformed.

### **3.2 Charlies Gulch Region**

Charlies Gulch is a 200 m deep gully in the southern coast of Dudley Peninsula, located 30 km directly south of Penneshaw. A 3 km long coastal

---

---

section surrounding Charlies Gulch exposes Kanmantoo metasediments interpreted by Dailey et al (1979) as the Petrel Cove Formation (fig. 12a). The coastal outcrop here is characterized by asymmetric parasitic flexural folds, faults, and an abundance of *en-echelon* veins.

Flexural folds in the Charlies Gulch region have steep axial planes, striking  $045^{\circ}$ , with fold axes that plunge  $15^{\circ}$ SW (fig. 12b). A cleavage is developed axial planar to these folds, which dips steeply towards the SE. The plunge of the flexural folds is to the SW, opposite in direction to the majority of folds seen on the NE coastline of the Dudley Peninsula (Map 1).

The strike of the flexural folds observed near Charlies Gulch, is sub-parallel to the strike of parasitic folds observed in the mapped region on the NE coast of Dudley Peninsula (Map1). Parasitic folds within the CBA, and buckle folds south of the SISZ, within the Carrickalinga Head Formation, have NW striking fold axial planes.

A fault is developed through the Charlies Gulch region, which strikes parallel to the cleavage, possibly representing brittle slip of a flexural fold.

In the region near Charlies Gulch, there is an abundance of vertical *en-echelon* tension gash veins that strike  $\sim 1$

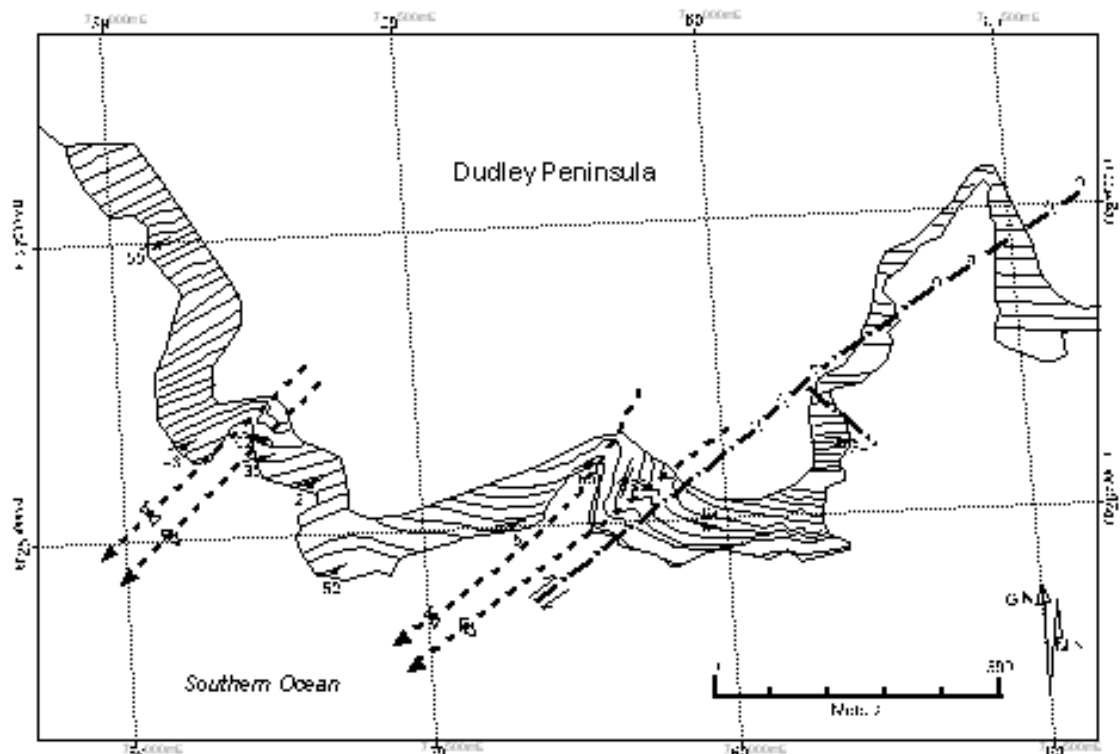


Fig. 12(a) - Coastal outcrop map, west of Charles Gulch, on the south coast of Dudley Peninsula, showing the orientation of bedding, and the outcrop traces of parasitic folds and faults.

| LEGEND |                        |
|--------|------------------------|
|        | Psammitic unit         |
|        | Pelitic Unit           |
|        | Fault                  |
|        | Anticline axial trace  |
|        | Syndinal axial trace   |
|        | Bedding strike and dip |

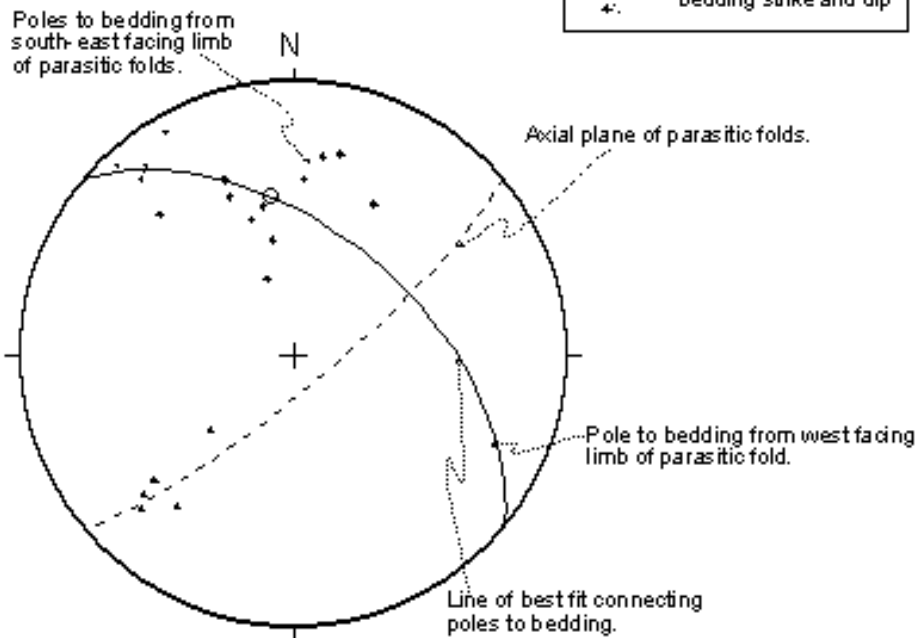


Fig. 12(b) - Equal area lower hemisphere stereographic projection, showing the relationship between poles to bedding (diamonds) from alternate limbs of parasitic folds, bedding/cleavage intersection lineations (triangles), and cleavage measurements (crosses) from the Charles Gulch region (Fig. 12 a). Note. The line of best fit is drawn between the mean of bedding poles from the SE facing limb (circle) to the pole to bedding from the west facing limb of the parasitic folds. The axial plane was determined by the line of best fit between the centre of the two fold limbs and the fold axial traces.

---

---

## 4. ANALYSIS OF BOUDIN, VEIN, AND FOLD GEOMETRIES

### **4.1 Boudinage analysis**

A representative analysis of boudins was conducted within the SISZ, at a location 150 m south of Sprigg Inlet, where perpendicular sections show differing boudin types. A cliff face section shows structural features representing the XZ plane of the local finite strain ellipsoid, and a wave-cut platform section shows structural features representing the YZ plane of the local finite strain ellipsoid.

Within the cliff face section, quartzite layers display shearband-type boudins, with individual boudins consistently rotated slightly ( $\sim 2^\circ$ ) towards the foliation, which is slightly oblique (at a higher angle) to the bedding planes (fig. 14). The boudins are rotated antithetically to the general SE over NW shear, with synthetic displacement along the interboudin surface. The consistency of these observations from cliff outcrops within the SISZ makes these boudins a reliable shear sense indicator (Goscombe and Passchier, in prep.). A single deformation is recorded by these boudins, indicating SE over NW movement.

The minimum extension of two quartzite layers from a location 150 m north of Sprigg Inlet was calculated by reconstructing boudin trains from digitised field photos using the constant area balance method (Lacassin et al. 1993) (fig. 13). This method yielded a mean minimum extension of each recorded quartzite layer to be 171% (see appendix 1).

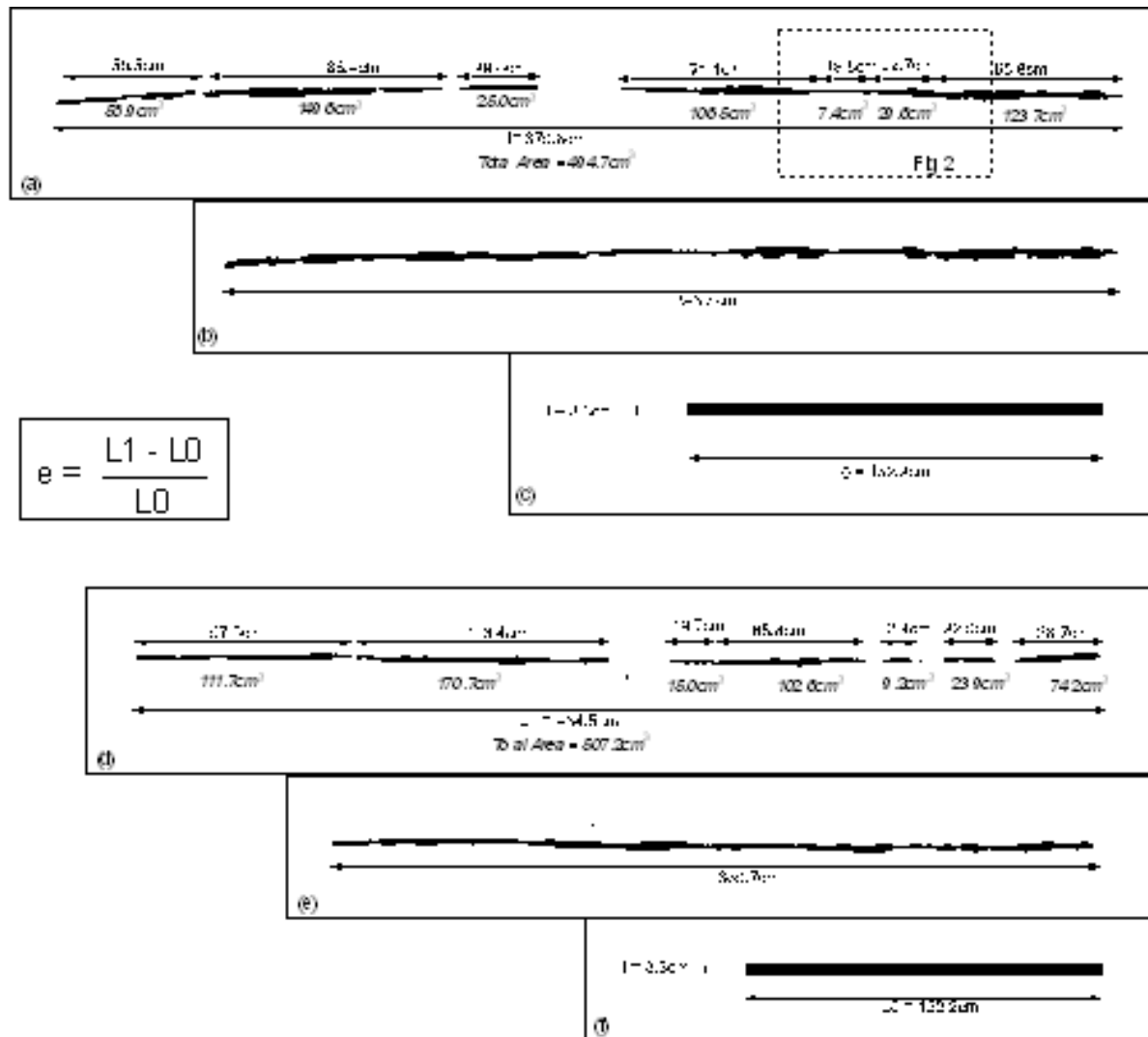


Fig. 13 - Reconstruction of boudinaged quartzite layers in north east facing cliff section 150 meters south of Sprigg Inlet. Recorded layers (a) and (d) are reconstructed to pre-isolation of boudin components (b) and (e), and to the calculated original layer prior to extension (c) and (f).

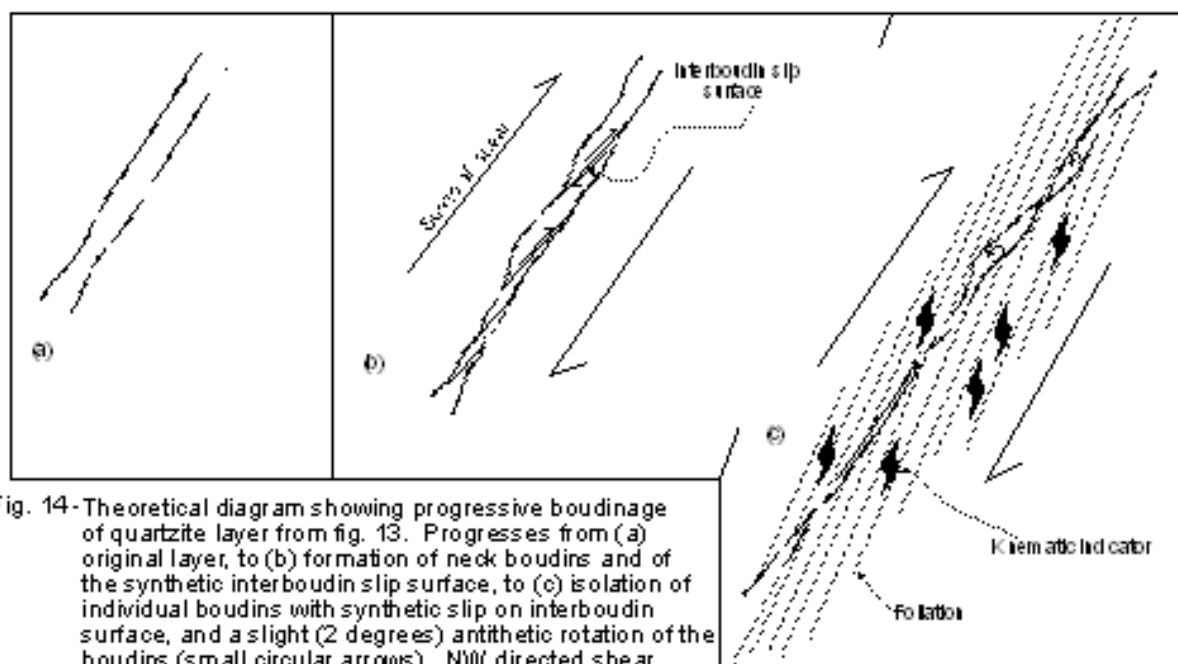


Fig. 14 - Theoretical diagram showing progressive boudinage of quartzite layer from fig. 13. Progresses from (a) original layer, to (b) formation of neck boudins and of the synthetic interboudin slip surface, to (c) isolation of individual boudins with synthetic slip on interboudin surface, and a slight (2 degrees) antithetic rotation of the boudins (small circular arrows). NW directed shear shown by large arrows. Quartzite layer and the foliation are in the true orientation as observed in the cliff face within the SISZ. Kinematic indicators are winged andalusite porphyroblasts indicating NW directed shear.

---

---

On the wavecut platform (XY plane), quartzite layers show drawn boudins and ramp folded structures (Goscombe and Passchier, in prep.), the latter of which is indicative of multiple deformation events. There is an abundance of interboudin vein fill, including sygmoidal gash veins. The shape of the sygmoidal curve of these veins was recorded in two opposing orientations, which provides evidence of strike-slip movement in 2 directions (fig. 15).

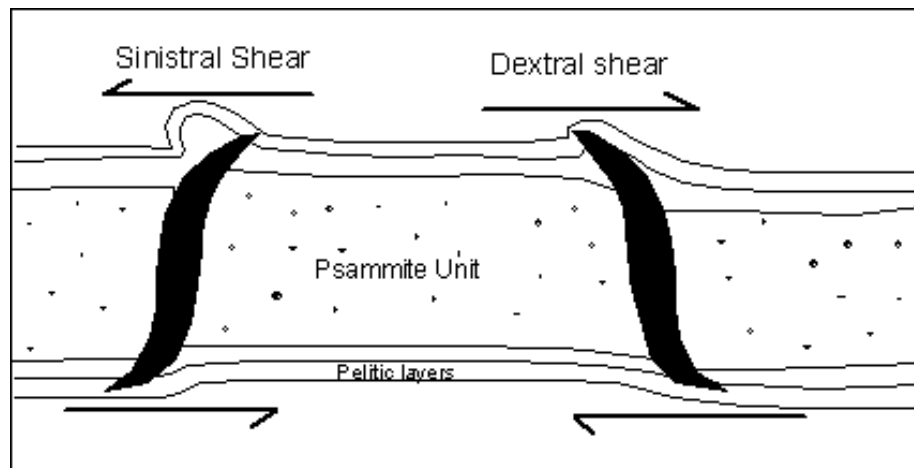


Fig. 15 – Representative diagram of sygmoidal interboudin quartz vein fill, as observed on the YZ plane at a location 150m east of Sprigg Inlet. Shear direction (arrows) is inferred from the geometry of the sygmoidal veins.

#### **4.2 Vein Analysis**

The three dimensional orientation of sygmoidal *en-echelon* vein arrays are reflective of the stress field active during brittle-ductile deformation of the host rocks (Ramsay and Huber, 1987; Smith, 1996). There are three possible mechanisms of formation of the *en-echelon* veins from the SISZ, dependant upon the relative timing of development of each vein set and the stress conditions from which they developed.

The three dimensional orientations of a N-S striking (sinistral) and E-W striking (dextral) set of tension gash veins within psammite layers were recorded from a location 50 m south of Sprigg Inlet. Stereographic

---

---

projections show the relationship of these veins to bedding and the inferred stress fields that may have produced these vein orientations.

*Mechanism 1 - VEIN DEVELOPMENT IN DIFFERENT STRESS REGIEMES*

In both coaxial and non-coaxial flow, tension gashes open approximately parallel to the direction of maximum instantaneous extension (or minimum compressive stress -  $\sigma_3$ ) (Passier and Trouw, 1998). During initial shear displacement, fissures are orientated perpendicular to the maximum instantaneous extension (Ramsay and Huber, 1987). Veins open in response to a maximum compressive stress ( $\sigma_1$ ) orientated parallel to the tips of the veins. The tips of the veins are orientated at  $135^\circ$  from the shear zone boundary (assuming no component of non-coaxial deformation). In this analysis it was assumed that bedding controlled shearing, thereby, the bedding planes hosting the veins define the localised shear zone boundary. From this the stress regime active during formation of the vein sets can be analysed (fig. 16).



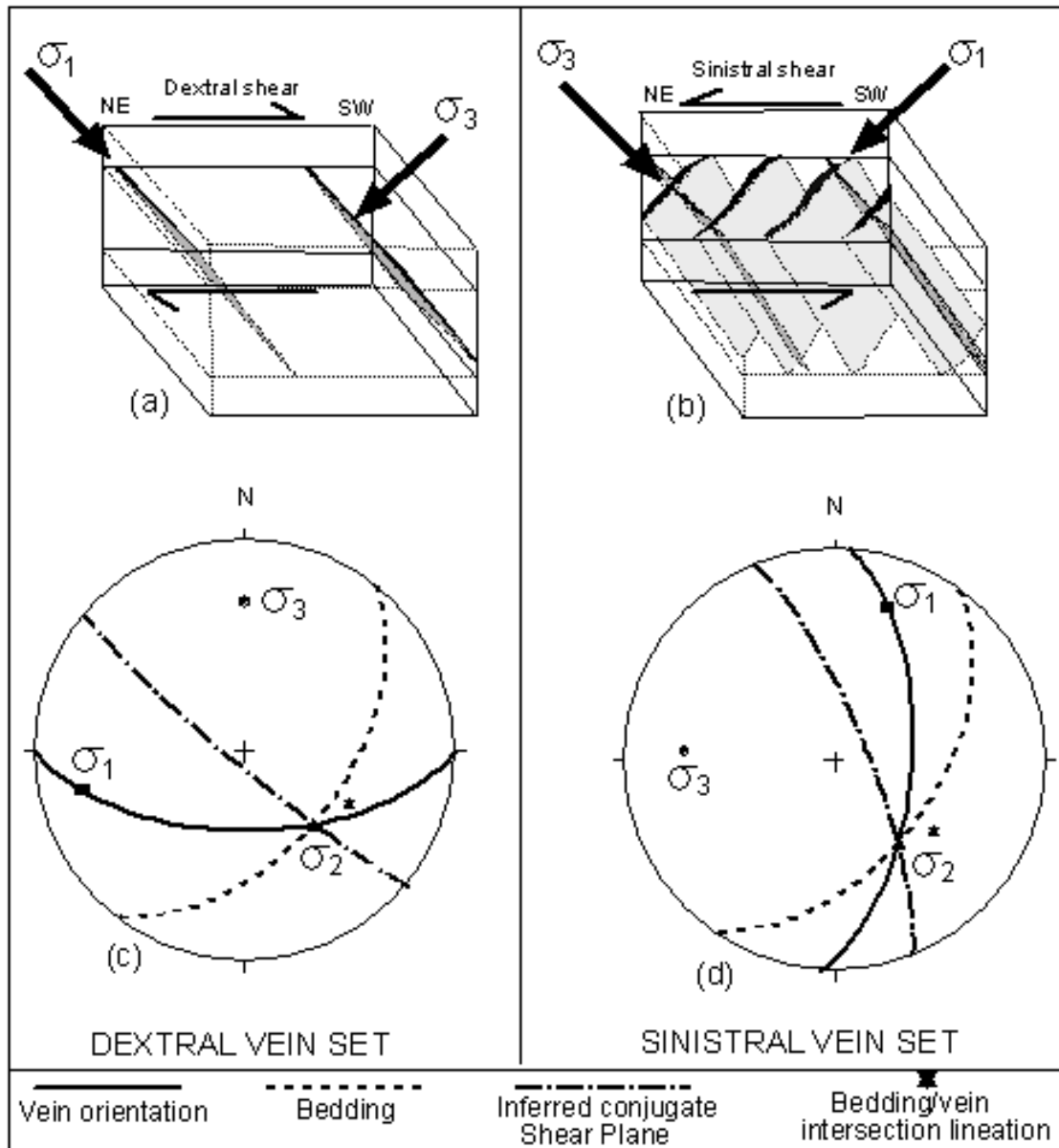


Fig. 16 – Inferred stress conditions producing the cross-cutting vein sets within psammite layers in the SISZ. Cartoons (a) and (b) show the orientation and stress conditions during formation of (a) dextral and (b) sinistral vein sets. Lower hemisphere stereographic projections show the orientation of stress conditions during formation of the (c) dextral and (d) sinistral vein sets.  $\sigma_1$ =Maximum compressive stress,  $\sigma_2$ =Intermediate compressive stress,  $\sigma_3$ =Minimum compressive stress.

This analysis shows that at some point during deformation, the maximum and minimum compressive stress switched through 90°, with the intermediate compressive stress ( $\sigma_2$ ) remaining consistent throughout.

---

---

### Mechanism 2 – PROGRESSIVE DEVELOPMENT DURING SIMPLE SHEAR

Extensional fissures open in response to the stress conditions as shown in the initial vein orientation from mechanism 1. That is, fissures initially open at  $135^\circ$  to the local shear direction (assuming homogeneous simple shear with no component of non-coaxial strain, see fig. 17a -A). As subsequent displacements take place within the local shear zone, the veins are rotated to an angle depending on the amount of subsequent shear strain (fig. 17a -B) As the veins open during progressive shear, they form as a parallel *en-echelon* array. When the shear displacement is large, the central part of the vein cannot extend further. At this stage new cross-cutting veins are developed (Fig. 17a -C).

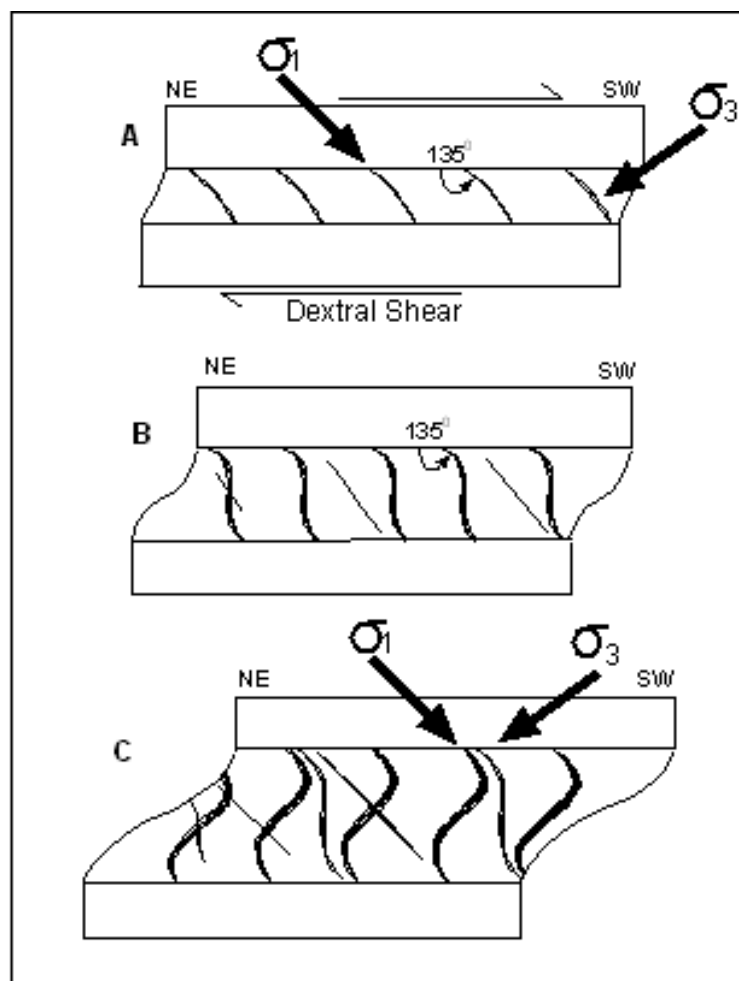


Fig. 17 (a) – Cartoon model showing formation of *en-echelon* vein sets during progressive simple shear. Adapted from Ramsay and Huber (1983).

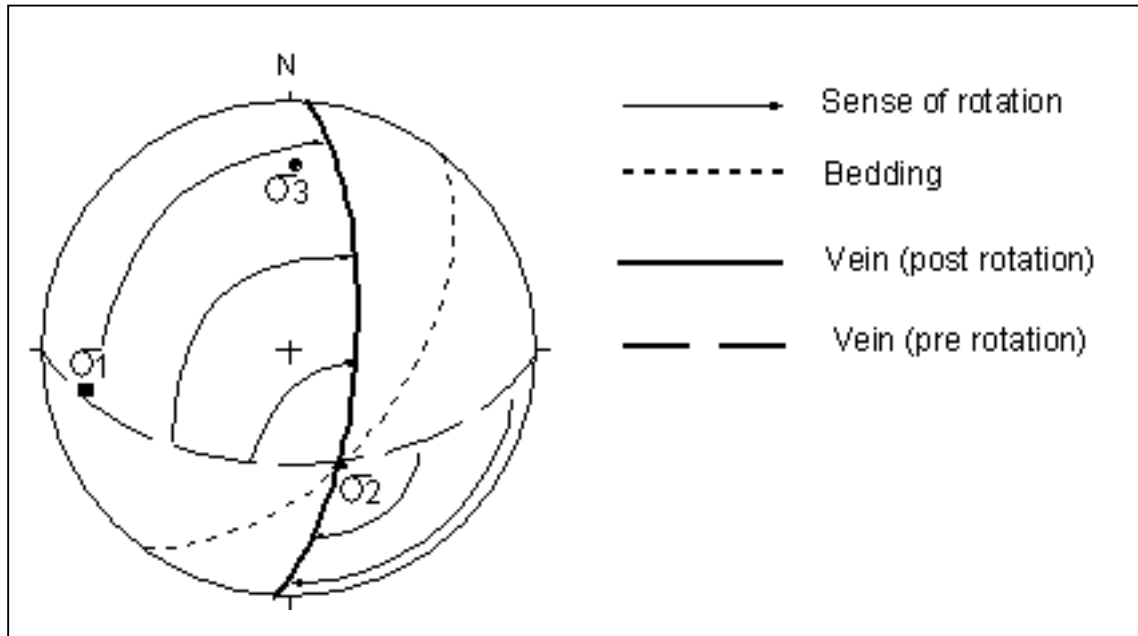


Fig. 18 - Lower hemisphere stereographic projection showing rotation of an initially E-W striking vein through 90° to a N-S orientation. Stress conditions are consistent throughout.

The dextral vein set observed within the SISZ, possibly represents the formation of cross-cutting veins as the abundant sinistral vein set was rotated (fig. 18).

### Mechanism 3 – VEINS DEVELOPED AS A CONJUGATE ARRAY

Alternatively the dextral and sinistral *en-echelon* vein sets could have formed simultaneously as a conjugate array. Conjugate arrays of veins were not obvious within the SISZ, possibly due to folding of veins within pelitic layers and the restriction of *en-echelon* veins within quartzite layers of up to 20 cm thickness. In conjugate vein arrays, one vein set often becomes dominant

over the other as shearing progresses (Ramsay and Huber 1987), possibly explaining the dominant abundance of the sinistral vein set within the SISZ.

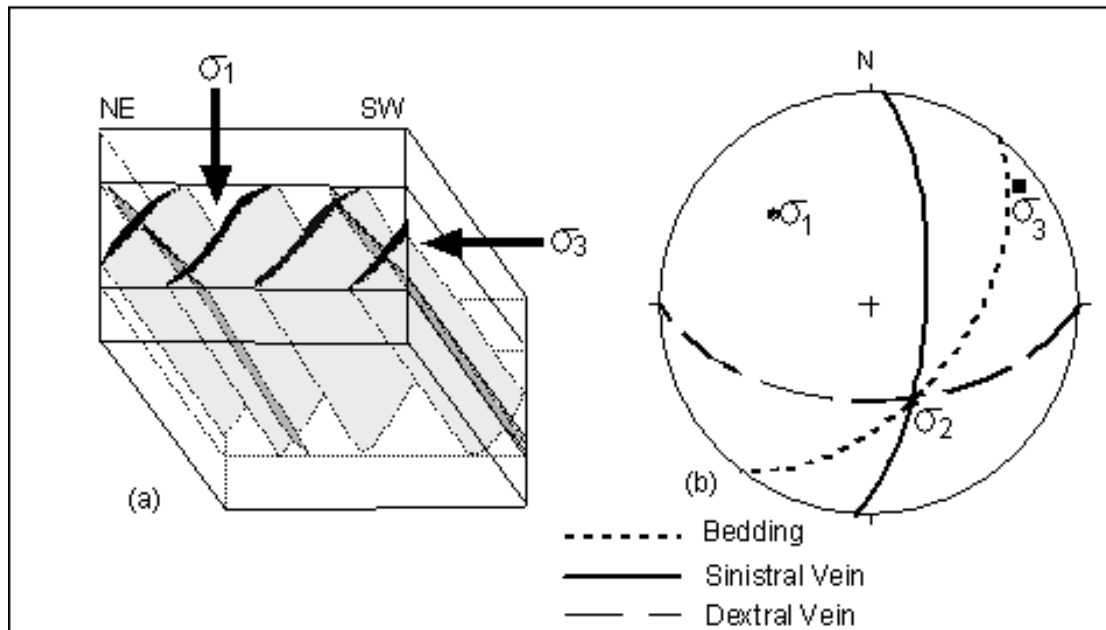


Fig. 19 – (a) Three-dimensional block diagram showing representation of sinistral and dextral vein sets from the SISZ. (b) Lower hemisphere stereographic projection showing the orientation of the stress conditions during formation of the conjugate vein sets.

The local stress that possibly produced the conjugate en-echelon vein arrays is orientated with the maximum compressive stress almost perpendicular to bedding (fig. 18).

### **4.3 Fold Analysis**

Huddleston analysis of folds within the SISZ show that there is a variation in the homogeneous flattening strain within the shear zone, with a concentration of flattening strain surrounding both the northern and southern boundary of the shear zone (Appendix 1, fig. 7). Huddleston analysis of a folded quartz vein, 20 m NW of the southern boundary of the shear zone, recorded the highest degree of post-buckle flattening strain throughout the mapped region. Reconstruction of a folded quartzite layer at the same location shows the layer has undergone 50.3% total shortening.

---

---

The highest recorded total shortening throughout the mapped region on the NE coast of Dudley Peninsula was observed by reconstruction of parasitic class 1c upright folds developed close to the axial plane of the CBA (fig. 2), which yielded 58.5% total shortening. Within the SISZ, reconstruction of a quartz vein observed 50 m south of Sprigg Inlet, recorded 44.4% total shortening.

#### **4.4 Discussion**

Deformation within the SISZ was not homogeneous. The SISZ is an asymmetric shear zone as identified by analysis of folds, which show variations of relative post-buckle flattening throughout the shear zone. The most intense flattening strain is associated with the boundaries of the SISZ. The interpretation of this is that the margins of the shear zones acted as thrust zones during NW directed shear. The NW boundary of the SISZ displays a sub-horizontal lineation, possibly reflecting strike-slip movement during transpression.

Shear directed to the NW within the SISZ is confirmed by the consistent lineation direction ( $45^{\circ} \rightarrow 120$ ), shearband-type boudins, and kinematic indicators that specify SE over NW shear (more precisely ESE over WNW shear). However, sequential boudins developed along strike, and a crenulation developed within the SISZ, gives evidence of two deformation events.

A dextral strike-slip component of deformation is associated with the initial WNW directed bulk shear. Along strike, quartzite units were boudinaged due to this strike slip movement, which possibly resulted from a plane strain component of deformation within the SISZ. The asymmetry of folds enveloping quartzite boudins observed on the YZ plane from the SISZ, indicates a sinistral strike-slip shear produced compression, which post-dates the dextral strike-slip shear which produced extension. The latter strike-slip

---

---

event produced folded boudins along strike within the SISZ, and also produced the crenulation observed at a few locations within the area mapped.

Crenulations in the area mapped were not readily identified or convincingly obvious. Yet they have been noted at several locations in this, and previous studies. Notably, near the Dudley Fault, within Sprigg Inlet, north of Sprigg Inlet, on the northern boundary fault of the Snapper Point Shear Zone, and at a location south of Snapper Point as previously mapped by Menpes (1992). All these locations are high strain zones within the mapped area, and all are in close proximity to, or within fault zones.

The stress conditions active during deformation have been analysed by the orientation of vein sets within the SISZ. The relationship between N-S striking (sinistral) and E-W striking (dextral) *en-echelon* vein sets within the SISZ gives rise to three possible models of deformation, dependant on the stress regime from which they developed.

MODEL 1 – Separate deformation events, and therefore different stress regimes, controlled the development of the sinistral and dextral *en-echelon* vein sets.

The dominant abundance of the *en-echelon* vein set that strikes N-S (sinistral vein set) is inconsistent with the bulk WNW directed shear. Since, if the shear is controlled along the bedding planes, then the effective stresses would not produce veins developed with a N-S strike. Rather the prominent shear direction is more conducive towards development of upright veins that strike WNW. Upright veins that strike E-W were observed from the Dudley Fault Zone and the SISZ, which possibly were developed during WNW directed shear (see chapter 4.2, mechanism 1).

---

---

At some point in time, the maximum compressive stress changed 90° in orientation to be directed towards the north. This change in the stress regime is consistent with the development of sequential boudins developed along strike within the SISZ, and the development of a crenulation with a lineation (L2) parallel to the mineral lineation (L1). Hence, the deformation producing the N-S striking veins is related to a regional deformation active towards the north, which resulted in sinistral strike-slip shear within the SISZ.

A problem exists in this model in that the dominant foliation within the SISZ is developed at 90° to the sinistral (N-S striking) *en-echelon* veins. Thereby, the development of this foliation is likely to have occurred at the same time as the formation of the sinistral vein set. However, winged strain shadows around andalusite porphyroblasts which define SE over NW kinematics and are aligned with the foliation, contradictory to the foliation formation during sinistral strike-slip shear.

MODEL 2 – Problems arising from model 1 can be, in part, solved with a model by which a single deformation event produced the *en-echelon* vein sets. In this model, rotation of initially E-W striking veins occurred during progressive strike-slip shear. A later E-W striking vein set formed after significant (90°) rotation of the initial veins (see chapter 4.2, mechanism 2).

This model effectively explains the perpendicular orientation of the two vein sets. This improved model also adequately explains the alignment of winged strain shadows around porphyroblasts with the foliation generated during NW directed shear. This model also explains the dominant abundance of the N-S striking vein set, in that the present E-W striking vein set formed late in the deformation event, after the initial vein set was rotated.

---

---

However, this model cannot explain the orientation of the foliation, which is perpendicular to the N-S striking vein set in the SISZ. Furthermore, this model cannot explain the existence of sequential boudins, or the crenulation observed within the SISZ. Folding of boudins and development of the crenulation must have occurred due to a different deformation event to that which produced the *en-echelon* vein sets.

MODEL 3 – The N-S striking and E-W striking vein sets formed as a conjugate array in a single deformation event, with the N-S striking vein set developed dominantly. The foliation is developed coevally with the deformation, adequately explaining the alignment of winged strain shadows around porphyroblasts, and the orientation of the N-S striking veins to the dominant foliation. A possible explanation for this is the stacking of thrust sheets during NW directed deformation, which produced intense flattening strain within the SISZ. This theory is supported by the inferred stress conditions ( $\sigma_1$ -  $30^\circ \rightarrow 315$ ) derived from the orientation of the *en-echelon* conjugate vein arrays.

However, this scenario cannot effectively explain the existence of sequential boudins along strike within the SISZ, or the development of a crenulation. A sinistral strike-slip deformation within the SISZ, which post-dated the onset of NW directed shear, must have occurred due to regional stresses acting outside the shear zone.

All of the models described above require two deformation events to adequately explain the formation of the structural features observed within the SISZ. The preferred model for vein development is model 3, which adequately explains the orientation of the vein sets to the dominant foliation. Also the inferred stress field which produced the formation of the vein sets is consistent with NW directed shear. Post-dating the onset of NW directed shear is a sinistral strike-slip component of deformation.



---

---

The relative magnitude of the two deformation events is evident from reconstruction of quartzite boudins, and from boudin types identified within perpendicular sections from the SISZ. It is clearly apparent that dip-slip extension associated with shear-band type boudinage far exceeds the dextral and sinistral strike-slip components of deformation.

## **5. MAGNETIC INTERPRETATION OF THE DUDLEY PENINSULA**

Magnetic anomalies on the Dudley Peninsula are in two forms, structurally controlled and stratigraphically controlled. The orientation of bedding was recorded at 20 locations on coastal and inland outcrops throughout Dudley Peninsula. These trends coincide with the trend of magnetic anomalies at 18 of these locations, indicating the magnetic signature of the Kanmantoo Group is closely related to bedding in this area, possibly due to the growth of magnetite during metamorphism. Thereby, the interpretation of bedding and fold axial traces is considered possible for the sub-surface geology of Dudley Peninsula.

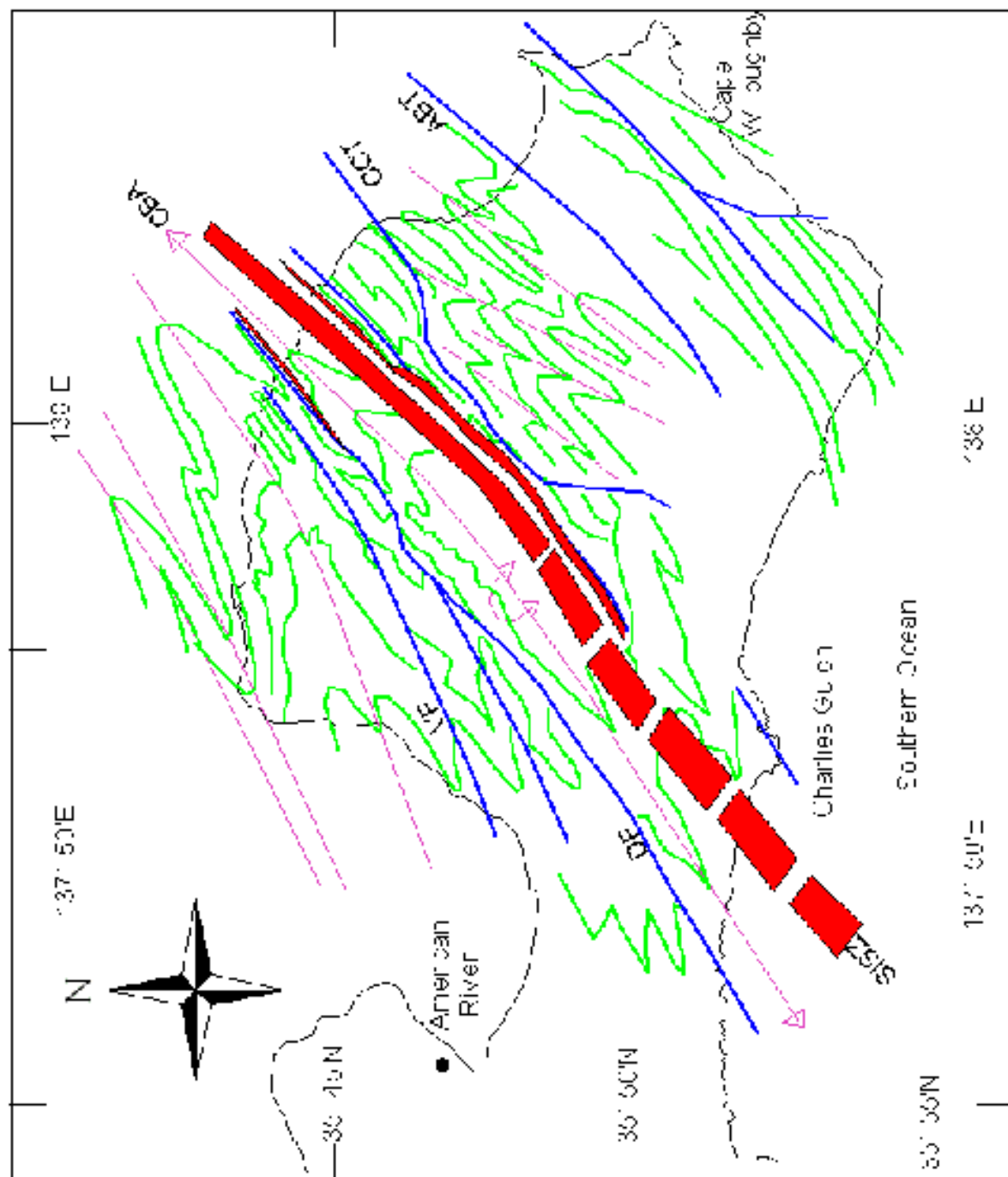
Magnetic anomalies can occur due to magnetite formed within high temperature shear zones, and in high strain zones between rocks of contrasting competency (Maidment and Gibson, 1999). Also, movement of fluids through a rock results in the destruction of magnetite, which also will create an anomaly. These factors all have implications for the interpretation of the magnetic data from Dudley Peninsula.






Magnetic anomalies are weak on the Dudley Peninsula, apart from three strong anomalies, one centred at Sprigg Inlet, another centred ~300 m north of Cuttlefish Bay, and another within the centre of Antechamber Bay. The weak anomalies are enhanced by the application of a vertical derivative filter to the data, thereby allowing the traces of folds, faults, and shear zones to be interpreted (fig. 20).

---

---

This interpretation shows tight folding produced significant shortening of Kanmantoo sediments on Dudley Peninsula. The interpretation of folds fits convincingly to previously mapped folds on the west coast of Dudley Peninsula (Flottmann and James 1997), and near Antechamber Bay (Menpes 1992). The axial trace of the CBA can be seen to trend NW with only a slight change in orientation. From this interpretation and field evidence, the CBA is double plunging, with a change in plunge occurring ~5 km SW of Cuttlefish Bay.



-  Shear Zone
-  Thrust Fault
-  Bedding trace
-  Fold Axial Trace
-  Contour line

CDA = Cuddeleys Day Anticline  
 CCT = Cape Cod Thrust  
 ACT = Antecape Cod Day Thrust  
 SISZ = Spragg Inlet Shear Zone  
 DF = Dudley Fault  
 VF = Vernor Fault



Fig. 20. - Interpretation of magnetic isochrons and tectonic features on the Cape Cod peninsula, showing the map view distribution of folds, faults and shear zones.

---

---

On Dudley Peninsula, NW of the CBA, fold axial traces diverge, and become more open to the west with fold axial traces bending from 045° in the north to 035° in the west. Offsetting these folds are the Vernon Fault, which trends 035°, and the Dudley fault which trends 045° in the north to two branches in the south trending 035°. From these observations, it is apparent that these reverse faults have a distinct relationship to fold development.

Southeast of the CBA, the most prominent feature is a straight positive anomaly trending 045° which intersects the coastline ~200 m south of Snapper Point. This anomaly extends for 15 km almost to the southern coast of the Dudley Peninsula. Fold axial traces are oblique either side of this anomaly, thereby separating structurally independent zones. Folds north of the anomaly trend NE to SW, whereas south of the fault, folds trend NNE to SSW. The consistently straight nature of this anomaly and the difference of fold orientations either side of it imply the interpretation of this feature as a structural anomaly.

Another straight positive magnetic anomaly is centred within Antechamber Bay, which also trends 045°. Folds are developed on the NW side of this anomaly, whereas to the SE, magnetic units are linear, and field evidence confirms that bedding is uniform in this area. Due to the similar style of this anomaly to anomalies centred on known thrust faults, and the difference in deformation style either side of this anomaly, I interpret this feature to be a thrust fault, and is termed here the Antechamber Bay Thrust.

The geographical extent of the SISZ is interpreted from the regional extent of structural features on Dudley Peninsula. Firstly, the CBA which trends NE to SW, within which the SISZ is developed in its southern upright limb. Secondly, by the parallelism of the Dudley and Vernon faults with fold axial traces, and thirdly by the long straight positive anomaly extending through the peninsula.

---

---

These observations lead to the interpretation of the SISZ to extend from Sprigg Inlet on the NE coast of Dudley Peninsula to cross the south coast ~2 to 3 km west of Charlies Gulch.

## **6 DISCUSSION**

### **6.1 Regional comparisons**

The proposed regional trace of the SISZ, and the CBA, is consistent with the orientation of thrusts and shear zones on southern Fleurieu Peninsula, and the orientation of folds on western Kangaroo Island (fig. 21).

There is a definite continuation of the orientation of the axial trace of major folds from 045° on southern Fleurieu Peninsula, through Dudley Peninsula, to 035° on western Kangaroo Island. The orientation of the CBA axial trace bends from 045° on the NE coast of Dudley Peninsula, towards the orientation of the fold axial traces of 4-8 km wavelength anticlines and 2-4 km wavelength synclines on western Kangaroo Island. The geometry of these folds on western Kangaroo Island suggests folding is related to faulting with only minor displacement (Flottmann et al. 1995). Impingement of sediments onto the SE corner of the Gawler Craton during the first phase deformation (NW directed) of the Delamerian Orogeny, resulted in more intense deformation in the area of Dudley Peninsula. More intense strain in the area of Dudley Peninsula is evident by the tightness of the CBA, compared with folds on western Kangaroo Island. Intense stress led to significant thrusting on both limbs of the CBA.

Flexural folds observed on the south coast of Dudley Peninsula, have a parallel fold axial trace and similar structural style to folds on the western and southern parts of the Fleurieu Peninsula, including asymmetric flexural folds at Parsons Headland (c.f. James, 1989). Similarly, the cleavage direction remains fairly consistent throughout the Dudley Peninsula and on the southern Fleurieu Peninsula (c.f. Johnson 1991, Rogers 1991), striking 040 to 050, and dipping steeply to the SE.

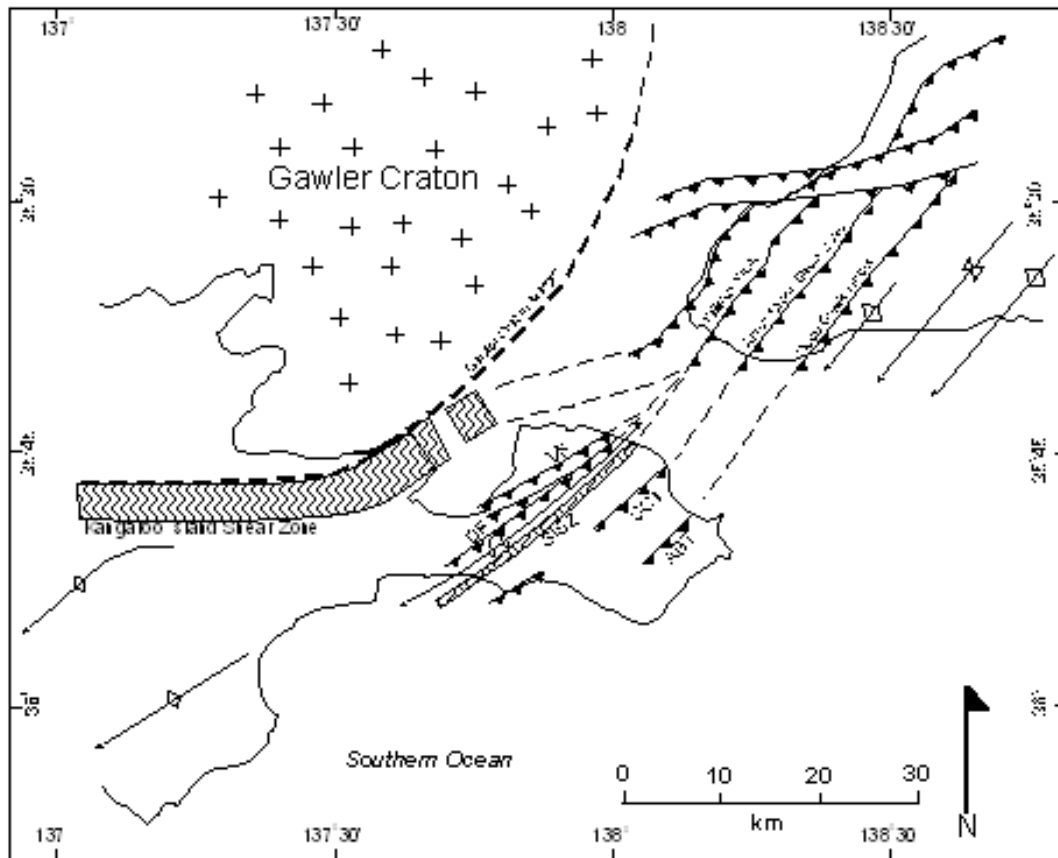


Fig. 21 - Renewed interpretation of structural features on Dudley Peninsula with possible comparisons to structural features on southern Fleurieu Peninsula.  
 ABT - Antechamber Bay Thrust, CCT - Cape Coutts Thrust, SISZ - Sprigg Inlet Shear Zone, DF - Dudley Fault, VF - Vernon Fault.

Direct comparisons between the SISZ to shear zones on southern Fleurieu Peninsula are not clear, however the degree of shortening calculated within a short section within the CBA (54%) is similar to the maximum shortening between the Talisker Fault and the Aaron Creek Shear Zone (57%) on southern Fleurieu Peninsula.

An elongate magnetic anomaly centred at Antechamber Bay trends 045°, and has a similar style to anomalies centred over the SISZ and shear zones on southern Fleurieu Peninsula. A straight-line theoretical continuation (consistent with other structural features in the area) of this anomaly on to southern Fleurieu Peninsula connects it directly with the Deep Creek Thrust.

---

---

## **6.2 Movements during deformation**

Structural relationships within the SISZ indicate the shear zone has been subjected to two deformation phases. The initial deformation involved top to the WNW bulk shear sense, followed by a less intense deformation involving sinistral strike-slip movement within the SISZ.

Strike-slip movements related to transpression are well documented (Sanderson and Marchini, 1984; Jones and Tanner, 1994; Goodwin and Williams, 1996). Models have been developed to show the effects of strain partitioning within transpressive shear zones, resulting in down dip, and strike-slip components during deformation. These models and the majority of field studies show the strike-slip displacement to be in consistent direction with the transpressive shear.

Strike-slip movements in opposing direction to the dominant transpressive shear direction are not common in fold-thrust belts, yet have been noted. In Dias and Ribeiro's (1994) study of the Ibero-Armorican arc in Portugal, they showed that there is a wide range of strain ellipsoids within transpression zones if lateral change, axial depression and volume change are taken into account. They found that within an inner zone near the hinge of the arc, constrictive ellipsoids occurred, along with *en-echelon* quartz veins that implied stresses opposing the general transpressive shear direction.

Stauffer and Lawry (1993) studied the Needle Falls Shear Zone within the Canadian Shield, reporting structures that rotate into the shear zone contrary to the direction predicted by ideal dextral simple shear. They interpreted this effect to reflect significant non-coaxial strain across the shear zone.

## **6.3 Tectonic models**

The structural grain throughout Dudley Peninsula does not define a major bend in plan view. Fold axial traces, fault traces, and cleavage measurements show only a slight ( $\sim 5^\circ$ - $10^\circ$ ) curve from the NE coast to the

---

---

south coast of Dudley Peninsula. This slight curve most likely reflects impingement of sediments onto the Gawler Craton during the first phase deformation of the Delamerian Orogeny.

The foliation within the SISZ was developed during the initial NW directed shear, which also produced boudinage, and initiated the formation of conjugate vein arrays. Within the SISZ, dextral strike-slip movement accompanied the NW directed transpression as initially straight fold hinges and thrust faults were bent slightly around the SE corner of the Gawler Craton.

The second deformation, as recognised from sinistral strike-slip movement within the SISZ, could be due to either;

- (a) Progressive bending of the fold-thrust belt around the SE margin of the Gawler craton during NW directed compression (fig. 22(c1) – MODEL 1),  
or,
- (b) due to a regional deformation active towards the north (fig 22(c2) – MODEL 2).

Reports by Stauffer and Lawry (1993) and Dias and Ribeiro (1994) indicate non-coaxial strain can produce extension in opposing direction to the expected extension direction during transpression. In the case of the SISZ, non-coaxial strain is caused by the stacking of thrust slices due to buttressing of Kanmantoo and Adelaidean sediments on to the SE corner of the Gawler Craton during the Delamerian Orogeny. Huddleston analysis has revealed that up to 35% homogeneous flattening strain has occurred in the SISZ. The analysis of vein geometries within the SISZ also supports this theory.

The emplacement of thrust sheets producing the majority of the bulk flattening strain within the SISZ occurred during NW directed compression (fig. 22b). Compression against the SE margin of the Gawler Craton resulted in a 5-10°



---

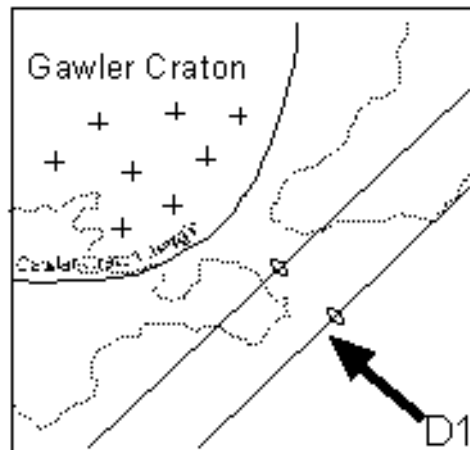
---

plan-view bend of folds, thrusts and shear zones in the region of Dudley Peninsula. Deformation within the SISZ involved a dextral strike-slip component prior to bending of the fold-thrust belt. At some point in time the component of strike-slip deformation changed from dextral to sinistral.

This change in direction of deformation is attributed to continual bending of the Fleurieu Arc during NW directed compression. As the fold belt was bent, a point of inflexion on the SE margin of the Gawler Craton marked the change in the strike-slip component of deformation, from sinistral in the Fleurieu limb, to dextral in the Kangaroo Island limb of the Fleurieu Arc. This inflexion point possibly corresponds to the point of maximum convergence of sediments onto the SE corner of the Gawler Craton during NW directed compression. With continual bending of the fold-belt, the inflexion point migrated towards the SW (fig. 22 (1c)). At some time during the late stages of NW directed compression, the inflexion point moved sufficiently far enough to the SW, to produce sinistral strike-slip movement within the SISZ.

An alternative model involves two separate regional deformation phases. The initial phase involved NW directed compression which produced the majority of structures within the Southern Adelaide Fold-Thrust Belt (fig. 22b). A second regional deformation phases was active towards the north on the southern parts of the Southern Adelaide Fold-Thrust Belt. This phase of deformation produced sinistral strike-slip movement within the SISZ.

## Alternative models for formation of the Fleurieu Arc



(a) above - Folding

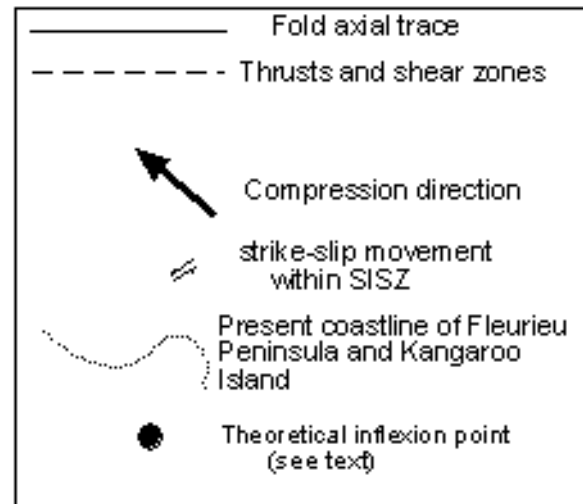
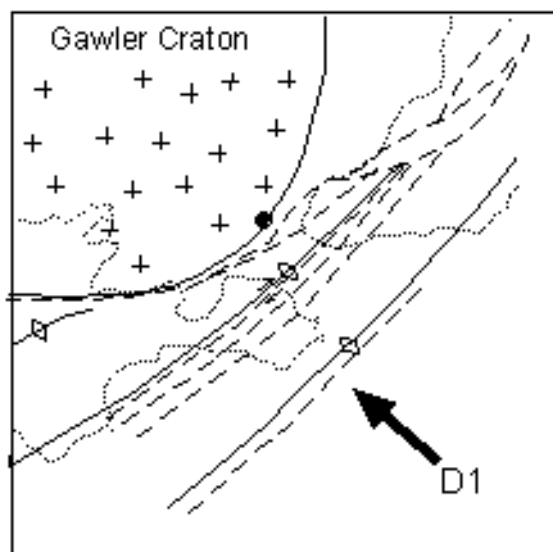
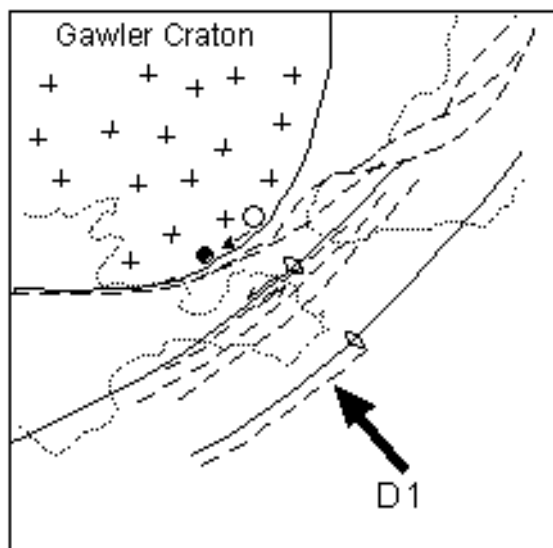


Fig. 22 - Models of formation of the Fleurieu Arc. SISZ = Sprigg Inlet Shear Zone. Inferred Gawler Craton Margin adapted from Belperio & Flint (1992).

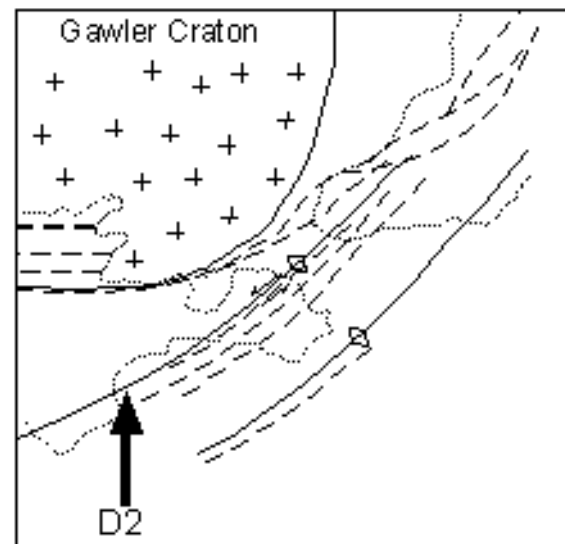


(b) left - Shear and thrust development. Basement involved thrusting on Fleurieu Peninsula. Thin-skinned deformation on Kangaroo Island. Note point of inflexion of strike-slip movement direction located near the present day Fleurieu Peninsula. Dextral strike-slip movement in SISZ.



### MODEL 1

(c1) Continuous deformation model. Fold belt is bent slightly around SE margin of Gawler Craton. Point of inflexion migrates SW with continual bending of the fold-belt. Sinistral strike-slip movement in SISZ.



### MODEL 2

(c2) Separate deformation model. Northerly directed compression results in slight bending of the Fold-thrust belt, development of thrusts on northern Kangaroo Island, and sinistral strike-slip movement in the SISZ.

---

---

A second (less intense than the first) phase of regional deformation directed towards the north on Kangaroo Island has previously been proposed by Marshak and Flottmann (1996). They described the Fleurieu Arc to be an orocline, which resulted from continual bending of foreland propagating thrusts and shear zones, with the latest movement being north directed compression. The model in this study is consistent with a late northerly movement during deformation.

The structural grain on Dudley Peninsula does not define a major bend in plan view, and there is no evidence of rotation of structural segments on Dudley Peninsula as proposed by Marshak and Flottmann (1996). For this reason I propose the Fleurieu Arc is essentially a primary arc as proposed by Flottmann and James (1997). Sinistral strike-slip movement within the SISZ was caused by curvature of the SAFTB around a theoretical inflexion point, which corresponds with the point of maximum convergence onto the SE margin of the Gawler Craton.

## 7. CONCLUSIONS

- The Sprigg Inlet Shear Zone is an asymmetric shear zone, with both basal and upper boundary thrust margins.
- The Sprigg Inlet Shear Zone and the structural grain on Dudley Peninsula defines a minor ( $\sim 5^\circ$  to  $10^\circ$ ) bend from  $045^\circ$  on the NE coast to  $\sim 040^\circ$  to  $035^\circ$  on the south coast.
- Structures within the Sprigg Inlet Shear Zone record two phases of deformation. The first resulted in the formation of boudins, conjugate *en-echelon* vein arrays, and fabric development with the general WNW bulk shear sense. The second deformation involved sinistral strike-slip shear within the Sprigg Inlet Shear Zone, which resulted in crenulation of the slaty cleavage (S1) and folding of boudins along strike.

- 
- 
- The sinistral strike-slip movement within the SISZ was caused by either;-  
  
-Impingement of NW directed deformation onto the SE corner of the Gawler Craton resulted in continual bending of the Fleurieu Arc, thereby changing the stress regime within the Sprigg Inlet Shear Zone to accommodate sinistral strike-slip shear.  
OR,  
-A regional deformation event active on the southern part of the Southern Adelaide Fold-Thrust Belt, which was active towards the north.
  - The structural grain is continuous throughout southern Fleurieu Peninsula, and Kangaroo Island. First generation deformation features define the structural grain of the Fleurieu Arc, and there is no evidence of a change in the strike of segments within the fold-belt. Therefore, the Fleurieu arc is classified as a primary arc, with possibly a minor component of oroclinal bending due to a later north directed deformation active on Kangaroo Island.

### **ACKNOWLEDGEMENTS**

I gratefully acknowledge the advice, criticisms and general supervision received from Dr Pat James during this difficult year. Sincere thanks are also extended to Wayne Mussard for thin sectioning and casual conversation. Thanks also go to Andy Burt of the Department of Primary Industries of South Australia, for supplying magnetic data, and helpful discussions.

Special thanks go to everyone who kept me sane when I was stressed, including Ben, Labba, Liza, and Geoff.

Finally I would like to thank my family for their help throughout the year, and above all Isobel for her love and support.

---

---

## REFERENCES

- Belerio A.P., Flint R.B.** (1992). The southeastern margin of the Gawler Craton. *Australian Journal of Earth Sciences*, **40**, 423-426.
- Belerio A.P., Preiss W.V., Fairclough M.C., Gatehouse C.G., Gum J., Hough J., Burt A.** (1998). Tectonic and metallogenic framework of the Cambrian Stansbury Basin – Kanmantoo Trough, South Australia. *AGSO Journal of Australian Geology and Geophysics*, **17**(3), p183-200.
- Carey S.W.** (1955). The orocline concept in geotectonics. *Proc. R. Soc. Tasmania*, **89**, p255-289.
- Clarke G.L., Powell R.** (1989). Basement/cover interaction in the Adelaide Fold Belt, South Australia: the development of an arcuate fold belt. *Tectonophysics*, **158**, p208-226.
- Daily B., Milnes A.R.** (1971). Discovery of Late Precambrian tillites (Sturt Group) and younger metasediments (Marino Group) on Dudley Peninsula, Kangaroo Island, South Australia. *Search* **2**, p431-433.
- Daily B., Milnes A.R.** (1972). Significance of basal Cambrian metasediments of andalusite grade, Dudley Peninsula, Kangaroo Island, South Australia. *Search* **3**, p89-90.
- Daily B., Milnes A.R.** (1973). Stratigraphy, structure and metamorphism of the Kanmantoo Group (Cambrian) in its type section east of Tunkalilla Beach, South Australia. *Transactions of the Royal Society of South Australia*, **97**, p-213-242.
- Daily B., Milnes A.R., Twidale C.R., Bourne J.A.** (1979). Geology and geomorphology. In: Tyler M.J., Twidale C.R., Ling L.K., (eds.), *Natural history of Kangaroo Island*, Royal society of South Australia, Adelaide. p1-38.
- Dias R., Ribeiro A.** (1994). Constriction in a transpressive regime: an example from the Iberian branch of the Iberio-Armorican arc. *Journal of Structural Geology*, **16**(11), p1543-1554.

- 
- 
- Flint D.J., Grady A.E.** (1979). Structural geology of Kanmantoo Group sediments between West Bay and Breakneck River, Kangaroo Island. *Transactions of the Royal Society of South Australia*, **103**, p45-56.
- Flottmann T., James P.R., Rogers J., Johnson T.** (1994). Early Palaeozoic foreland thrusting and basin reactivation at the southeastern Palaeo-Pacific margin of the Australian Precambrian Craton: a reappraisal of the structural evolution of the Southern Adelaide Fold Thrust Belt. *Tectonophysics*, **234**, p 95-116
- Flottmann T., James P.R., Menpes R., Cesare P., Twinning M., Fairclough M., Randabel J., Marshak S.** (1995). The structure of Kangaroo Island, South Australia: strain and kinematic partitioning during Delamerian basin and platform reactivation. *Australian Journal of Earth Sciences*, **42**, p35-49.
- Flottmann T., Cockshell C.D.** (1996). Palaeozoic basins of southern South Australia: new insights into their structural history from regional seismic data. *Australian Journal of Earth Sciences* **43**, p45-55.
- Flottmann T., James P.** (1997). Influence of basin architecture on the style of inversion and fold-thrust belt tectonics – the southern Adelaide Fold-Thrust Belt, South Australia. *Journal of Structural Geology*, **19**(8), p1093-1110.
- Goodwin L.B., Williams P.F.** (1996). Deformation parth partitioning within a transpressive shear zone, Marble Cove, Newfoundland. *Journal of Structural Geology*, **18**(8), p975-990.
- Goscombe B.D., Passchier C.W.** Boudinage classification: Mechanisms of formation and evaluation as kinematic indicators, Kaoko Belt, Namibia. *In publication*.
- Hindle D., Burkhard M.** (1999). Strain, displacement and rotation associated with the formation of curvature in fold belts; the example of the Jura arc. *Journal of Structural Geology*, **21**, p1089-1101.
- Hudleston P.J.** (1973). Fold morphology and some geometrical implications of theories of fold development. *Tectonophysics*, **16**, p1-46.

- 
- 
- James P.R.** (1989). Field excursion guide – structural geology of the Fleurieu Peninsula. *SGTSG conference field guide*.
- Jenkins R.J.F., Sandiford M.** (1992). Observations on the tectonic evolution of the Southern Adelaide Fold Belt. *Tectonophysics*, **214**, p27-36.
- Johnson T.M.** (1991). The structure of the Blowhole Creek area, southern Adelaide Fold Belt, Fleurieu Peninsula, South Australia. University of Adelaide B.Sc. (Hons.) thesis, unpublished.
- Lacassin R., Leloup P.H., Tapponnier P.** (1993). Bounds on strain in large Tertiary shear zones of SE Asia from boudinage restoration. *Journal of Structural Geology*, **15**(6), p677-692.
- Maidment D. W., Gibson G.M.** (1999). Sources of magnetic anomalies in the Broken Hill Region, NSW. *Australian Geological Survey Organization (AGSO), Record no.6*.
- Mancktelow N.S.** (1990). The structure of the Southern Adelaide Fold Belt, South Australia. In: *The evolution of a Late Precambrian-Early Palaeozoic rift complex: the Adelaide Geosyncline*, eds Jago G.S., and Moore P.S., *Geological Society of Australia special publication*, **16**, p369-395.
- Marshak S.** (1988). Kinematics of orocline and arc formation in thin-skinned orogens. *Tectonics*, **7**(1), p73-86.
- Marshak S., Flottmann T.** (1996). Structure and origin of the Fleurieu and Nackara Arcs in the Adelaide fold-thrust belt, South Australia: salient and recess development in the Delamerian Orogen. *Journal of Structural Geology*, **18**(7), p891-908.
- McClay K.R.** (1997). *The mapping of geological structures*. Geological Society of London Handbook, John Wiley and sons, London.
- Offler R., Flemming P.D.** (1968). A synthesis of folding and metamorphism in the Mt Lofty Ranges, South Australia. *Journal of the Geological Society of Australia*, **15**, p245-266.
- Menpes R.** (1992). Structural evolution of a transpression zone in the Southern Adelaide Fold-Thrust Belt: northeast Dudley Peninsula,

- 
- 
- Kangaroo Island. University of Adelaide B.Sc. (Hons.) thesis, unpublished.
- Passchier C.W., Simpson C.** (1986). Porphyroclast systems as kinematic indicators. *Journal of Structural Geology*, **8**(8), p831-834.
- Passchier C.W., Trouw R.A.J.** (1998). *Microtectonics*. Springer, Berlin.
- Preiss W.V.** (1987). The Adelaide Geosyncline – Late Proterozoic stratigraphy, sedimentation, palaeontology and tectonics. *Geological Survey of South Australia, Bulletin* **53**.
- Ramsay J.G., Huber.** (1983). *The techniques of modern structural geology. Volume 1: Strain analysis*. Academic press, London.
- Ramsay J.G., Huber.** (1987). *The techniques of modern structural geology. Volume 2: Folds and fractures*. Academic press, London.
- Rogers J.R.** (1991). The structure of the Talisker area, southern Adelaide Fold Belt, Fleurieu Peninsula, South Australia. University of Adelaide B.Sc. (Hons.) thesis, unpublished.
- Sanderson D.J., Marchini W.R.D.** (1984). Transpression. *Journal of Structural Geology*, **6**(5), p449-458.
- Smith J.V.** (1996). Geometry and kinematics of conjugate vein array systems. *Journal of Structural Geology*, **18**, p1291-1300.
- Stauffer M.R., Lewry J.F.** (1993). Regional setting and kinematic features of the Needle Falls Shear Zone, Trans-Hudson Orogen. *Canadian Journal of Earth Sciences*, **30**, p1338-1354.
- Tikoff B., Greene D.** (1997). Stretching lineations in transpressional shear zones: an example from the Sierra Nevada Batholith, California. *Journal of Structural Geology*, **19**, p29-39.
- Yassaghi A., James P.R., Flottmann T.** (2000). Geometric and kinematic evolution of asymmetric ductile shear zones in thrust sheets, Southern Adelaide Fold-Thrust Belt, South Australia. *Journal of Structural Geology*, **22**, p889-912.



---

---

## APPENDIX 1

### Boudinage Reconstruction : Method

Field measurements and photographs were taken of 2 quartzite layers within a cliff section (XZ plane) at a location 150 meters south of Sprigg Inlet, to determine the degree of extension in this plane.

Field measurements were taken of the total length (L1) of the boudin trains and of individual boudins, together with the maximum width (t) of both of the quartzite layers.

Drawings of the boudin trains were traced from superimposed photographs, and digitised into ARCview format where the area of each boudin could be measured.

Each boudin train was then reconstructed using the constant area balance method (Lacassin et al, 1993). This method assumes the maximum thickness of the recorded boudinage train (t) to be the original thickness of the layer prior to extension, and that the area of the layer remains constant during deformation.

From this theory the layers were reconstructed to an original thickness (t) and length (L0). Hence an elongation (E) was determined according to the formula;

$$E = \frac{L1 - L0}{L0}$$

This gave a percentage elongation of 156% and 186% (Table X) for boudinage layers 1 and 2 respectively (mean 171%).

---

---

It should be kept in mind that this value gives a minimum constraint on the percentage elongation, as less competent pelitic layers would accommodate deformation more than quartzite layers. Also any flattening component or volume loss will give an underestimate of the maximum thickness (t) hence reducing the extensional value (e).

results: Table X – Results of boudinage reconstruction

|         | L1      | L0      | t     | e    | %e  | $\lambda$ |
|---------|---------|---------|-------|------|-----|-----------|
| Layer 1 | 379.8cm | 148.3cm | 3.3cm | 1.56 | 156 | 6.56      |
| Layer 2 | 434.5cm | 152.2cm | 3.3cm | 1.86 | 186 | 8.15      |

---



---

## APPENDIX 2 – FOLD ANALYSIS

### 1) HUDDLESTON METHOD (after Huddleston 19 )

This method yields an apparent X/Z value for the strain ratio, giving an indication of the flattening strain.

This method assumes folds of original class 1B are flattened to form class 1C folds. Two angles are measured from class 1C folds, either from field photographs taken looking down the plunge of the fold, or from tracings of folds done in the field, or from hand samples. The angles measured are;  $\theta$  = angle between an isogon and the normal to the parallel tangents of a folded surface of a layer to dip,  $\alpha$ .

These parameters are plotted on a graph with  $\alpha - \theta$  on the ordinate and  $\alpha$  on the abscissa. The slope of the line represents the specific x/z ratio as predetermined by huddleston. The ratio of  $\sqrt{\lambda_2/\lambda_1}$  can be read off the graph, and a % homogeneous flattening strain can be determined.

### RESULTS:

| Location                           | Section | Fold Host     | $\sqrt{\lambda_2/\lambda_1}$ |
|------------------------------------|---------|---------------|------------------------------|
| 100m NW of Sprigg Inlet            | YZ      | Quartzite bed | 0.45                         |
| 150m NW of Sprigg Inlet            | YZ      | Quartzite bed | 0.55                         |
| 200m NW of Sprigg Inlet            | YZ      | Quartz vein   | 0.53                         |
| 400m NW of Sprigg Inlet            | YZ      | Quartz vein   | 0.42                         |
| 500m NW of Sprigg Inlet            | YZ      | Quartz vein   | 0.31                         |
| Sample B4                          | YZ      | Quartzite bed | 0.60                         |
| 50m W of SISZ                      | YZ      | Quartzite bed | 0.69                         |
| 20m inside southern margin of SISZ | YZ      | Quartz vein   | 0.27                         |
| Sprigg Inlet                       | YZ      | Quartz vein   | 0.40                         |
| Sprigg Inlet                       | YZ      | Quartz vein   | 0.30                         |
| Cuttlefish Bay                     | XZ      | Sturt Tillite | 0.41                         |
| 100m South of Sprigg Inlet         | YZ      | Quartz vein   | 0.43                         |

---

---

## 2) FOLD RECONSTRUCTION METHOD

Folds were reconstructed to their initial unstrained length by calculating the strain imposed on the layer, initially creating buckling of the layer and secondly flattening of the buckled layer.

The flattening strain was calculated by the Huddleston method (described above). This was removed by stretching the sketch of the fold on Freehand8.0, keeping the area constant. The medial arc length (length of the fold measured from the center of the folded layer) of the fold was measured giving a value L0 – original length of the layer. Also measured is the direct length from the ends of the fold limbs from the original tracing (L1).

A percentage buckle shortening can then be calculated by using the formula;

$$\% \text{ Buckle shortening} = \frac{L1 - L0}{L0} \times 100$$

The total shortening of the layer is calculated by addition of the percentage homogeneous flattening as a percentage of the percentage buckle shortening with the percentage buckle shortening.

### RESULTS:

| Location                   | Fold Host     | %Buckle Shortening | %Homogeneous flattening | %Total shortening |
|----------------------------|---------------|--------------------|-------------------------|-------------------|
| 150m south of Sprigg Inlet | Quartzite     | 43%                | 17%                     | 50.3%             |
| Cuttlefish Bay (fig.X)     | Sturt Tillite | 43%                | 36%                     | 58.5%             |
| 50m south of Sprigg Inlet  | Quartz vein   | 33%                | 35%                     | 44.4%             |

---

---

## THIN SECTION DESCRIPTIONS

A1148/CC1 (XZ section) – Andalusite schist

Mineralogy – Biotite 80%, Quartz 15%, Andalusite 5%, Garnet 5%

Texture – Winged andalusite porphyroblasts up to 7mm in diameter retrogressed to biotite and quartz. Garnets show heclitic textures.

A1148/SP1 (XZ section) – Andalusite schist

Mineralogy – Biotite 63%, Quartz 30%, Andalusite 5%, Carbonate 2%

Texture – Andalusite porphyroblasts within fine grained biotite and quartz matrix. Porphyroblasts are up to 2cm long and 5mm wide and show retrogression to biotite and quartz.

A1148/SP8 (XY section) – Interbedded metapsammite

Mineralogy – Quartz 50%, Biotite 50%

Texture – Thinly bedded (~2mm beds) quartz +minor biotite, with biotite +minor quartz. Foliation defined by biotite parallel to bedding in biotite rich layers, but is refracted obliquely in quartz rich layers. Possible weak pre-existing foliation oblique to main foliation, also weak crenulation not well defined in quartz rich layers

A1148/SZ2 (XY section) – Massive quartzite

Mineralogy – Quartz 90%, Biotite 5%, Garnet 5%, +- heavy minerals

Texture – Matrix of fine grained quartz with garnet porphyroblasts. Coarse grained quartz within vein.

A1148/S3 (XY section) – Quartzite

Mineralogy – Quartz 70%, Biotite 20%, Garnet 5%, +- heavy minerals

Texture – Matrix of fine grained quartz, biotite and heavy minerals, with coarse garnet and biotite in close proximity to bedding parallel quartz vein.

Heavy mineral lamination defines bedding, biotite oblique to bedding defining

---

---

foliation, foliation curved from bedding parallel to 30 degrees inclined from bedding.

A1148/SN6 (XZ section) – Andalusite Schist

Mineralogy – Andalusite 40%, Biotite 30%, Quartz 30%, +minor Staurolite, +- heavy minerals

Texture – Pristine andalusite porphyroblasts up to 15mm with occasional retrogression spots of biotite. Heclectic textures within andalusite defined by heavy mineral inclusion. Fine grained quartz/biotite matrix.

A1148/SN5 (XY section) – Massive quartzite

Mineralogy – Quartz 80%, Biotite 10%, Garnet 5%, Cordierite 5%, Actinolite 2%, +- heavy minerals

Texture – Fine grained quartz, biotite matrix. Reaction rim surrounding 4 mm thick quartz vein, Cordierite in close contact with vein, biotite, garnet and actinolite within 1 to 2 cms from vein.

A1148/CB12 (XY section) – Layered actinolite-rich hornfels

Mineralogy – Actinolite 50%, Biotite 20%, Cordierite 20%, Scapolite 10%, +minor Garnet.

Texture – Layered mineralogy. Actinolite/cordierite layers with strongly anastomosing biotite. Biotite layers show preferred orientation of biotite parallel to layering. Remnant porphyroblasts (possibly andalusite) overgrown by biotite and later scapolite within biotite rich layers.

A1148/CB12 (XZ section) – Layered actinolite-rich hornfels

Mineralogy – as for XY section described above.

Texture – Early andalusite porphyroblasts show elongation, and are overgrown by biotite and scapolite. Foliation defined by biotite is deflected in biotite rich layers.

A1148/CB3 (XZ section) – Schist

---

---

Mineralogy – Quartz 45%, Scapolite 15%, Biotite 32%, Garnet 5%,  
Staurolite 3%, +- heavy minerals

Texture – Remnant mineral (possibly andalusite) formed pre-foliation generation shows pseudomorph texture defined by quartz and biotite. Matrix of fine grained quartz and biotite with porphyroblasts of, staurolite (syn-pre deformational), scapolite (syn-post deformational), and garnet (pre-deformational).

A1148/CB11 (XY section) – Actinolite schist

Mineralogy – Actinolite 35%, Scapolite 30%, Cordierite 10%, Quartz 10%,  
Biotite 5%, Staurolite 5%, Chlorite 5%, +- heavy minerals.

Texture – Mineralogical layering not well defined. Actinolite associated with cordierite. Staurolite always in contact with cordierite. Randomly orientated late scapolite overgrowths.

A1148/CB11 (XZ section) – Actinolite schist

Mineralogy – as for XY section described above.

Texture – layering 0.5 to 1cm thick. Matrix of fine grained quartz and biotite with randomly orientated actinolite.

A1148/CB7 (XZ section) – Actinolite schist

Mineralogy – Quartz 50%, Chlorite 15%, Biotite 10%, Actinolite 10%,  
Scapolite 10%, Staurolite 5%, +minor sulphides, +minor chlorite

Texture – Micro-quartz veins with actinolite and sulphides. Biotite defines weak foliation. Polymorph texture of remnant mineral replaced by quartz and biotite. Quartz/biotite layers altered to scapolite.

A1148/CB1 (XZ section) – Schist

Mineralogy – Quartz 40%, Biotite 40%, Garnet 5%, Actinolite 4%, Staurolite  
1%, +- heavy minerals

Texture – Matrix of very fine grained quartz and biotite defining a foliation. Sinistral quartz vein cross cuts foliation and contains quartz, biotite, with

---

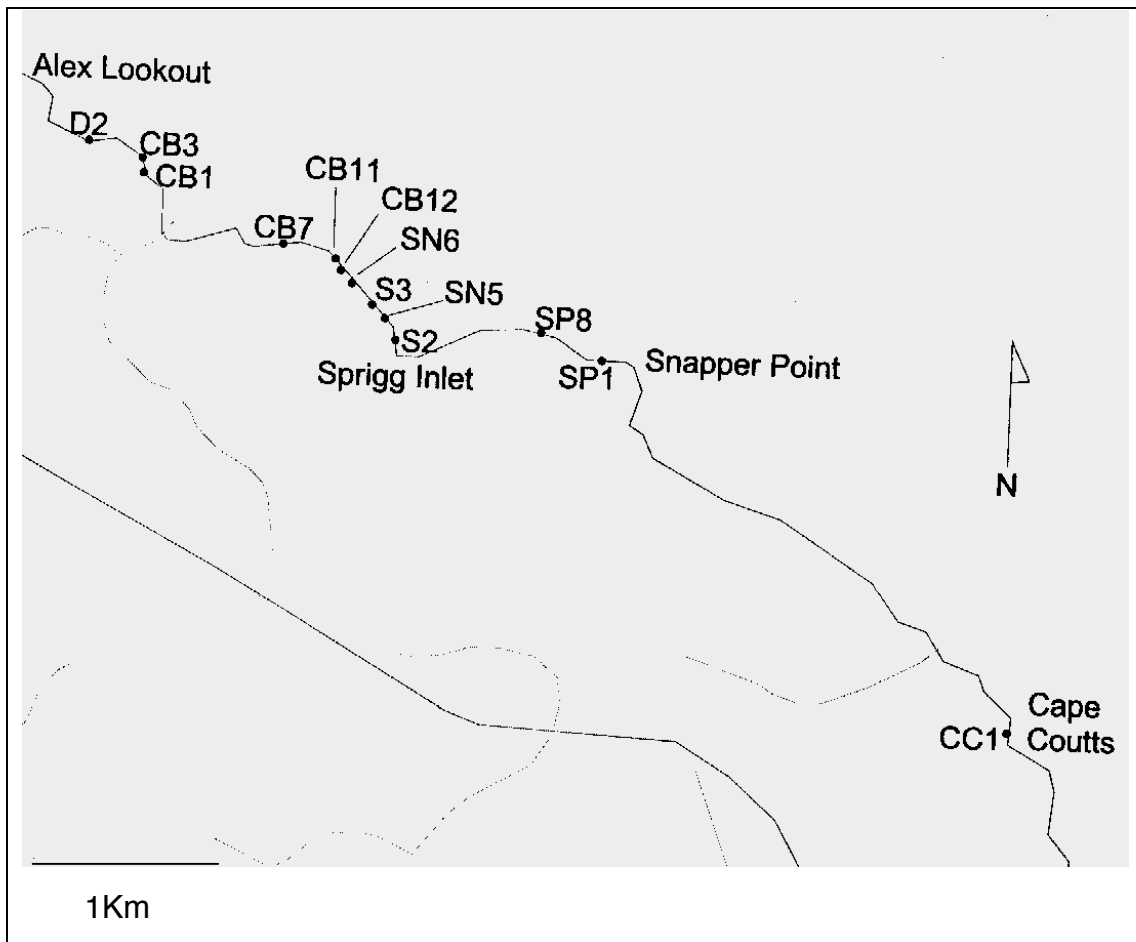
---

actinolite and staurolite central within the vein. Garnets in close proximity to vein show heclitic textures.

A1148/D2 (XZ section) – Andalusite schist

Mineralogy – Quartz 60%, Biotite 20%, Andalusite 15%, Heavy minerals 5%

Texture – Andalusite porphyroblasts up to 4 mm wide display kinematic indicators and heclitic textures. Fine grained quartz/biotite matrix.



Thin section localities on the NW coast of Dudley Peninsula, Kangaroo Island.